(2)

Unclassified
SECURITY CLASSIFICATION OF THIS PAGE

REPORT DOCUMENTATION PAGE

Form Approved
OMB No 0704-0188

1b RESTRICTIVE MARKINGS

AD-A219 403

3 DISTRIBUTION / AVAILABILITY OF REPORT
Approved for public release; distribution unlimited

4 PERFORMING ORGANIZATION REPORT NUMBER(S)
N00014-86-K-0316

5 MONITORING ORGANIZATION REPORT NUMBER(S)

6a NAME OF PERFORMING ORGANIZATION	6b OFFICE SYMBOL (If applicable)	7a NAME OF MONITORING ORGANIZATION
University of Arizona		Office of Naval Research

6c ADDRESS (City, State, and ZIP Code)	7b ADDRESS (City, State, and ZIP Code)
Department of Chemistry Tucson, AZ 85721	Arlington, Virginia 22217

8a NAME OF FUNDING / SPONSORING ORGANIZATION	8b OFFICE SYMBOL (If applicable)	9 PROCUREMENT INSTRUMENT IDENTIFICATION NUMBER
Office of Naval Research		N00014-86-K-0316

8c ADDRESS (City, State, and ZIP Code)	10 SOURCE OF FUNDING NUMBERS			
	PROGRAM ELEMENT NO	PROJECT NO	TASK NO	WORK UNIT ACCESSION NO
Arlington, VA 22217				

11 TITLE (Include Security Classification)
"Continued Investigations of New Concepts for Improved Spectrochemical Analysis"

12 PERSONAL AUTHOR(S)
M. Bonner Denton

13a TYPE OF REPORT	13b TIME COVERED	14 DATE OF REPORT (Year, Month, Day)	15 PAGE COUNT
Final Report	FROM 5/1/86 TO 4/30/89	January 5, 1990	100

16 SUPPLEMENTARY NOTATION

17 COSATI CODES			18 SUBJECT TERMS (Continue on reverse if necessary and identify by block number)
FIELD	GROUP	SUB-GROUP	Spectroscopy, analytical instrumentation.

19 ABSTRACT (Continue on reverse if necessary and identify by block number)

A strongly interlocking program designed to yield important new methodology for use in chemical analysis has been conducted. Fundamental investigations designed to gain new insight into areas of plasma spectroscopy through developing improved models of plasma discharges have been made. Studies which are contributing to a revolution in ultraviolet and visible detection have been conducted.

20 DISTRIBUTION / AVAILABILITY OF ABSTRACT	21 ABSTRACT SECURITY CLASSIFICATION
☒ UNCLASSIFIED/UNLIMITED ☐ SAME AS RPT ☐ DTIC USERS	Unclassified

22a NAME OF RESPONSIBLE INDIVIDUAL	22b TELEPHONE (Include Area Code)	22c OFFICE SYMBOL
M. Bonner Denton	(602) 621-8246	

DD Form 1473, JUN 86 — Previous editions are obsolete — S/N 0102-LF-014-6603

SECURITY CLASSIFICATION OF THIS PAGE
Unclassified

OFFICE OF NAVAL RESEARCH

FINAL REPORT

for

Contract N00014-86-K-0316

R&T Code 4131012---03

"Continued Investigations of New Concepts
for Improved Spectrochemical Analysis"

Principal Investigator: M. Bonner Denton
Professor of Chemistry

University of Arizona
Department of Chemistry
Tucson, Arizona 85721
(602) 621-8246

ABSTRACT

A strongly interlocking program designed to yield important new methodology for use in chemical analysis has been conducted. Fundamental investigations designed to gain new insight into areas of plasma spectroscopy through developing improved models of plasma discharges have been made. Studies which are contributing to a revolution in ultraviolet and visible detection have been conducted.

INTRODUCTION

An innovative research program which has addressed a number of significant problems in the field of spectrochemical analysis has been conducted.

During the course of this project, major advancements in numerous areas have contributed to an improved understanding of fundamental chemical processes as well as contributing toward improvements in chemical analysis and advanced instrumentation. The tremendous momentum established in many areas have resulted in major new achievements during the contract period. Technological spinoffs from many of the proposed investigations are contributing to our national science and technology as well as national security and defense.

Throughout the course of this project as number of "firsts" have been achieved. These include:

1. First application of Babington Principle Nebulization to spectrochemical analysis [1, 2].
2. First elemental analysis of organic compounds with an inductively coupled plasma [3].
3. First successful operation of a 27 MHz inductively coupled plasma in excess of 5 KW [4].
4. First operation of a demountable high vortex swirl ICP torch United States Patent No. 426G,113 [5, 6].
5. First hydride preconcentration technique for use with inductively coupled plasma [7].
6. First analysis of the effluent from a gas chromatograph with an inductively coupled plasma [8].

7. First empirical formula determination of organic effluents from a chromatograph with an inductively coupled plasma. United States Patent No. 4,293,220 [9, 10].
8. First observation of an inductively coupled plasma in the vacuum ultraviolet region below 170 nm [11].
9. First evaluation of Charge Injection Camera devices in the ultraviolet spectral region [12].
10. First quantitation of nonmetals in the vacuum ultraviolet region below 170 nm with an inductively coupled plasma [13].
11. First use of a heated high solids nebulizer for direct analysis of wear metals in oil [14].
12. First to demonstrate the improved accuracy and selectivity inherent in using an ICP for analyzing nucleotides separated by high performance liquid chromatography [15].
13. First theoretical comparison of various approaches for three dimensional mapping flames and plasmas employing Abel Inversion Concepts [16].
14. First operation and evaluation of an inductively coupled plasma at 150 MHz [17].
15. First totally windowless flowthrough cell for optoacoustic spectrometry [18].
16. First use of Iterative Coefficient Weighted Least Squares Technique for improved mixture analysis employing optoacoutic spectrometry [18].
17. First to mix destructive and nondestructive readout capabilities on a charge injection device (CID).
18. First use of a CID for atomic spectroscopic analysis.

19. First to achieve simultaneously variable pixel to pixel integration periods on a CID and apply this capability for improved dynamic range.
20. First three dimensional mapping of vacuum ultraviolet emission profiles in an ICP.
21. First application of "thinned" charge coupled devices to terrestrial chemical analysis.
22. First use of an inverted inductively coupled plasma for improved particulate analysis.
23. Elucidation of ion transmission characteristics of RF only quadrupolar fields ("total" ion transmission mode has been shown to mass dependent in a complex manner) [19].
24. First demonstration of sweeping mass in the notch filter (RF only mode) of a quadrupole mass filter using RF amplitude.
25. First evaluation of effects of torch size on plasma stability and ability to accept sample aerosol at 150 MHz [17].
26. First evaluation of excitation phenomena as a function of pressure [20].
27. First to operate high voltage hollow anode-cathode discharges in the United States.
28. First to evaluate the potential of high voltage hollow anode-cathode discharges as spectroscopic sources.
29. First to demonstrate the use of the Denton microchannel plate nebulizer for efficient sample nebulation with greatly reduced sample carryover.
30. First to retrofit a commercial ICP torch system for high pressure operation.

31. First to operate single element Charge Injection Device.
32. First to demonstrate rapid spectral acquisition in one and two spatial dimensions using a CCD [21].
33. First to contrast QE of deep depletion vs. standard depletion CCDs, with and without antireflection coatings.
34. First to produce images from 2048 x 2048 resolution CCD imaging detector.
35. First demonstration of selective photoionization of drugs from complex matrices demonstration production of only molecular ions [22].
36. First to demonstrate the ability to jump to different wavelengths to increase dynamic range.
37. First to propose a mechanism for the crosstalk phenomenon for CIDs and to show that it is not due to charge transfer from detector element to detector element.
38. First to demonstrate superior fluorescence detection with a CCD [23].
39. First to demonstrate ultra-trace chemiluminescence determined with a CCD [24].
40. First to contrast analytical performance of CID detectors with CCD detectors [25].
41. First evaluation of real world performance of a holographic aberration corrected imaging spectrograph [26].
42. First to rigorously consider the potential of binning spectral images in a CCD [27].

43. First to demonstrate the analytical potential of spatially encoded Fourier transform spectroscopy from the ultraviolet to near infrared [28].

44. First to implement a crossed interferometric dispersive spectrometer and demonstrate its potential [29].

REVOLUTIONARY NEW DETECTORS FOR OPTICAL SPECTROSCOPY

Visible and ultraviolet optical spectroscopy today is one of the most widely employed analytical techniques used routinely to characterize the chemical and physical nature of an ever increasing range of materials for science and engineering.

During the last twenty years, most of the major improvements in absorption, fluorescence and emission techniques have involved development of better sources, absorption cells (including flames, furnaces, etc.), wavelength discrimination systems and data reduction methods (computers).

Very little progress has been made in the area of detectors (with the possible exception of photodiode arrays, which, it can be argued, are merely a Darwinistic precursor to the current generation of solid state devices). To be sure, over the years many workers have recognized the tremendous need for improved detectors. Unfortunately, the characteristics of the time-proven photomultiplier tube (PMT) have been difficult to out-perform. Characteristics including peak quantum efficiencies approaching 25%, dark currents of 100 down to 5 counts per second (in photon "counting" mode), linear dynamic ranges of over 10^6 and internal gains of over 10^6, have contributed to the PMT's wide acceptance (Please note that not all of these characteristics are simultaneously available, i.e., Photon counting mode cannot provide 10^6 dynamic range, quantum efficiency and noise characteristics are poor below 700 nm, etc.).

Unfortunately, the PMT is a single channel device. Numerous workers have explored a wide variety of television type electronic cameras to provide simultaneous or rapid sequential observation of a large number of wavelengths. These include the silicon vidicon [3,30,31], the silicon

intensified target (SIT) vidicon [32], the image dissector [3,33], the secondary electron conduction tube [5] and photodiode arrays [8,9].

Unfortunately, all of these devices have been found to suffer from one or more problems associated with poor dynamic range, spatial and temporal crosstalk (blooming and lag), insufficient number of resolution elements, poor quantum efficiency over the desired wavelength regions, high dark currents, high noise, high cost, poor mechanical properties, poor reproducibility, etc. Today multichannel applications are still forced to resort either to a scanning single channel PMT approach or to the use of multiple PMTs laboriously aligned to each of the wavelengths being observed (limiting the practical number of wavelengths which can be viewed). Recent advances in solid state detectors and support electronics hold great promise for changing this situation, not only in applications where simultaneous multiwavelength observations are desirable, but even in single channel systems.

During the course of this project, we have made considerable progress toward this goal including first demonstrating the ultraviolet response of Charge Injection Devices (CIDs) and the ability to vastly expand their dynamic range through judiciously mixing destructive and nondestructive readouts. We have developed techniques for characterizing many of the important parameters including sensitivity, linearity, noise, dynamic range, blooming, pixel crosstalk and spectral response to a degree of accuracy and precision vastly superior to the approach used by the manufacturers [34].

At this point in time it can safely be said that we know more about techniques for operating and characterizing the CID devices for "scientific" low light applications than anyone else in the world including the manufacturer, CID Technologies (CIDTEC). In fact, CIDTEC's confidence in our

capabilities developed under ONR funding is attested to through their continued supply of new and prototype devices (CID-17 BAS, CID-62, CID-20, CID-35) and our joint development of a new CID-75 single element detector designed to replace the photomultiplier tube in single channel systems (see Single Element Charge Injection Device section). Use of our knowledge has resulted in successful application of CID devices in atomic emission spectroscopy as well as additional improvements in atomic emission using a variety of sources including direct current and inductively coupled plasmas (see Atomic Emission section) as well as arc and spark.

While the CID currently offers unmatched performance in spectroscopic applications requiring extreme dynamic range (i.e., atomic spectroscopy), a second class of imaging array detectors, Charge Coupled Devices (CCDs), actually provide better performance at extremely low light levels and are currently available in higher resolution and larger silicon formats. Techniques which could most greatly benefit from these devices' capabilities include fluorescence, phosphorescence, and Raman spectroscopies. Unlike CIDs, we cannot claim to have learned more about operating CCDs in low light level imaging than anyone else in the world, however it is safe to say we are right in the middle of the fight. We have developed a better insight into their capabilities and potential in spectrochemical analysis than anyone else in the world. As a result of our developing reputation, connections with the manufacturers and other experts in the field necessary to exploit these devices have been developed.

Our expertise in the operation and optimization of CCDs, coupled with our knowledge of analytical spectroscopy, put us in a unique position to use the abilities of these new detectors to their greatest advantage in improving chemical analysis. The 2048 x 2048 element array is currently the

largest area (2-1/4" x 2-1/4") solid state detector in the world. Such a detector, with over 4 million individual sensing elements, combined with extremely low read noise and high QE, holds great promise for advances in simultaneous multielement atomic absorption analysis (continuum AA) (see Continuum Atomic Absorption section). CCD detectors also promise to revolutionize molecular spectroscopy. Linear CCDs promise to improve performance in molecular absorption measurements, allowing configurations of miniature, highly rugged portable systems (see section on Holographic Common Path Interferometric Spectrometers). A new technique for time resolved spectroscopy, called spectral framing [21], has been pioneered in these laboratories. The ability to simultaneously obtain complete spectra with a time resolution of 2 sec has great potential for phosphorescence measurements (see section on Time Resolved Spectroscopy Using a CCD in a Spectral Framing Mode).

Several factors make charge transfer devices (CCDs and CIDs) excellent detectors for molecular spectroscopy. Silicon detectors have excellent quantum efficiency in the ultraviolet and visible region of the spectrum far superior to the quantum efficiency of photomultipliers which rely on the ejection of electrons from photocathodes. High quality scientific CCDs have extremely low readout noises of between 10 to 50 electrons per charge packet readout. Charge transfer devices are capable of being cooled to 140 degrees K and below, which all but eliminates dark current and allows integration of photons for periods measured in hours. The high quantum efficiency, low dark current and readout noise give CCDs a higher signal to noise ratio for low light level applications than any other detector, including a photon counting photomultiplier tube. These detectors are solid state and employ no electron beam readout schemes; they are extremely rugged, compact, and

stable. CCDs are available in the widest array of imaging formats of any detector, from 128 element linear devices to 2048 by 2048 element two dimensional devices.

The use of both linear and two dimensional charge transfer devices for analytical spectroscopy has been limited to date. The reasons for this include the lack of commercially available scientific detector systems, the high cost and limited availability of devices and the large amount of computer memory necessary to handle the tremendous amount of data generated by these devices.

While charge transfer devices are available in home and commercial video cameras suitable for television applications, they are not widely available in so called "scientific" cameras. The scientific readout mode involves a number of factors including precise clocking of charge, double correlated sampling of the analog signal to remove KTC noise [35] and high precision digitization.

The average chemist's exposure to solid state devices has been limited to commercially available photodiode arrays (PDA) and detector systems from Reticon, PARR, Hewlett Packard, Perkin Elmer and LKB. Photodiodes have been very valuable in introducing many spectroscopists to multichannel detection systems, and in high light levels PDAs perform reasonably well. However, due to limited number of detector elements and the high read noise (greater than 1000 electrons for the best scientific devices) photodiode arrays are unsuitable for low light level detection. It should be noted that while some improvement in PDA technology can be expected to reduce the read noise of these devices, fundamentally the structure of a photodiode will always impose a lower noise limit that is one to two orders of magnitude larger

than the read noise of a CCD [36]. While photodiodes are commonly intensified to increase the signal above the read noise of the device, intensification is done at the expense of substituting the inherently broad spectral response of silicon with the limited spectral response and quantum efficiency of a photocathode. For example, with a CCD with 4 electrons of read noise, which is currently the lowest noise device we have evaluated, the dominant source of noise is photon shot noise after only a few photon absorption events. With read noise values this low, intensification is not only unnecessary but can be counterproductive by swapping the inherently high quantum efficiency of a silicon device with the lower quantum efficiencies of photocathodes.

While CCDs have the lowest read noise and largest formats of any detector, CIDs have several unique capabilities including a variety of specialized readout modes enabling CID technology to address the problems of analytical spectroscopy in ways that no other detector system can.

One unique feature of the CID is the ability to measure the photogenerated charge information contained within a detector element either by removing the charge or by leaving it undisturbed. These two read modes are called the destructive read mode and the nondestructive read mode [37,38]. The ability to mix destructive and nondestructive read modes from detector element to detector element distinguishes the CID from all other detectors. This ability has several advantages for analytical spectroscopy. The first is that individual detector elements may be interrogated as to how much photogenerated charge has accumulated while photons are still being collected. This is done without disturbing the charge information already stored. Based on the signal level measured, a decision can be made to either continue integrating photons or to read the signal level, store the

integration time, and then discontinue monitoring that particular site. This allows adjustment of the integration time from detector element to detector element to achieve near saturation conditions at every detector element and hence a maximum signal to noise ratio.

The second advantage is that the nondestructive read allows the reduction of the system read noise. The sources of system read noise in the CID include the first stage of the video preamplifier and several on-chip sources. A major component of the read noise is white or random, through reading the same charge information multiple times and averaging, the contribution of this component can be reduced. The effectiveness of this procedure is illustrated in Figures 1, 2, and 3 which show the results of tests performed using the CID-17 system constructed in these laboratories. Figures 1 and 2 show the effect of performing multiple nondestructive reads on signal level. Ideally, no change in signal level should be observed. The figures show that in fact a 0.1 percent shift is observed after performing 2000 nondestructive reads. Figure 3 shows the effect of performing nondestructive reads on system read noise. Read noise is reduced to 60 electrons from 950 electrons after 400 nondestructive reads.

There are a number of significant spectroscopic problems which are in need of simultaneous multiwavelength detectors with extremely high quantum efficiencies in the ultraviolet. These include high resolution line width measurements, multielement detection, VUV laser spectroscopy, etc. Unfortunately, most CCDs and photodiodes arrays (PDAs) do not have a high response for UV photons. One of the major reasons sighted for the decrease in quantum efficiency of CCDs in the UV-VUV region is the presence of overlaying gate electrodes on the surface of the CCD [37]. These polycrystalline silicon electrodes strongly absorb the UV light and thus reduce the

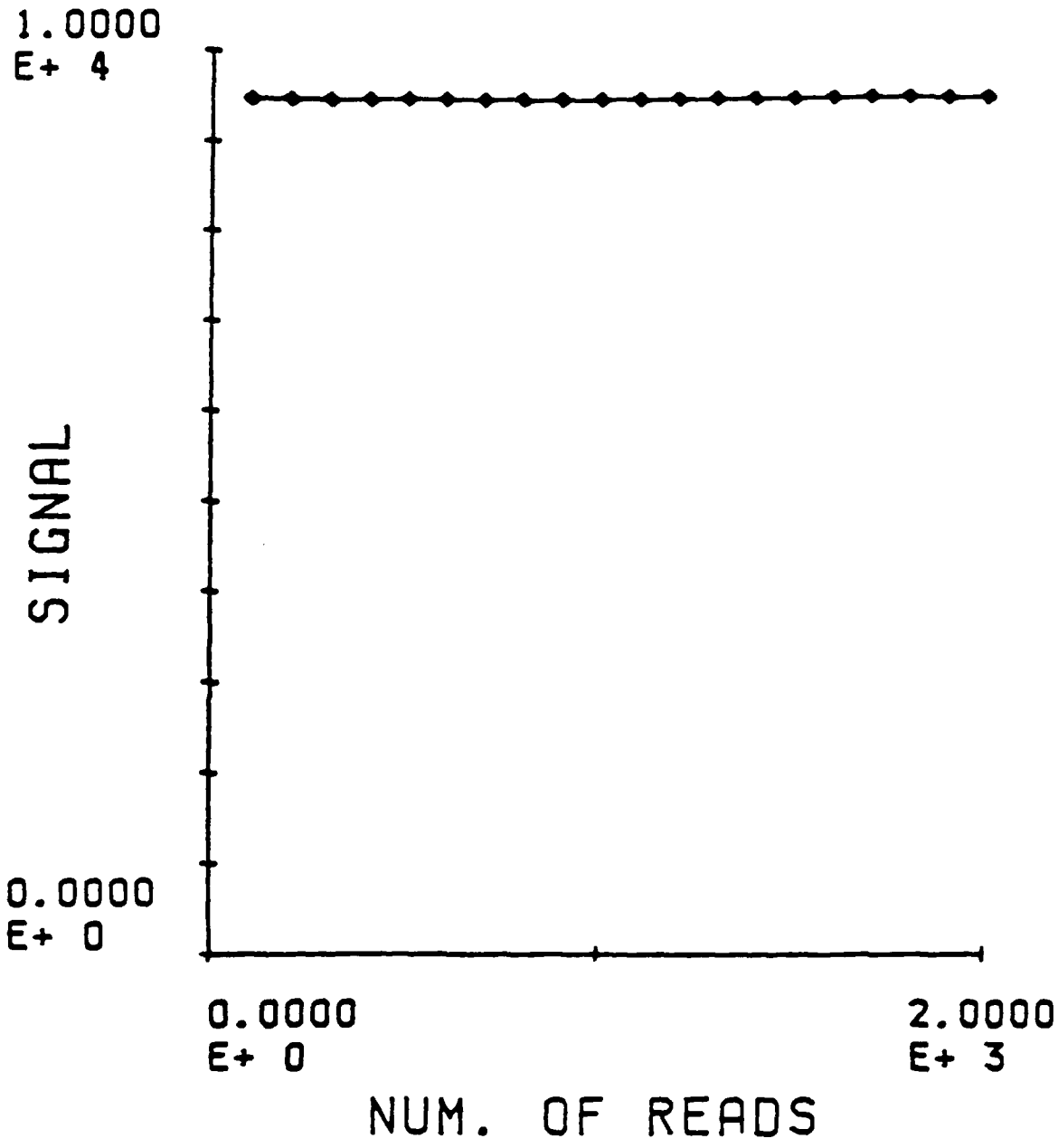

Figure 1
Effect of performing multiple nondestructive read outs (NDRO's) on signal level showing that percentage change is signal level is very slight.

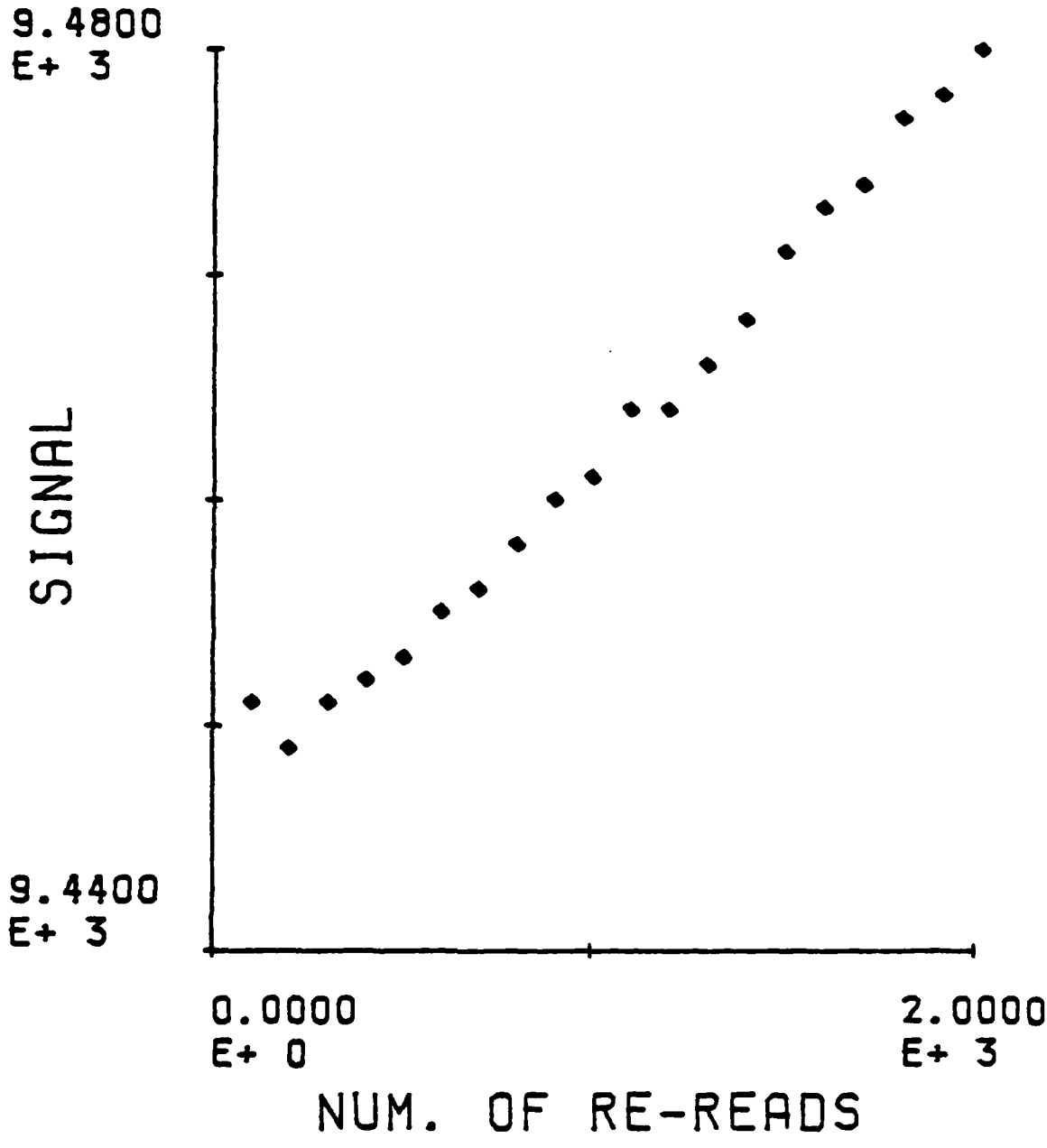

EFFECT OF RE-READS

Figure 2

Effect of performing multiple NDRO's on signal plotted on expanded scale showing 0.7 ppt increase in signal level after 2000 re-reads.

Figure 3

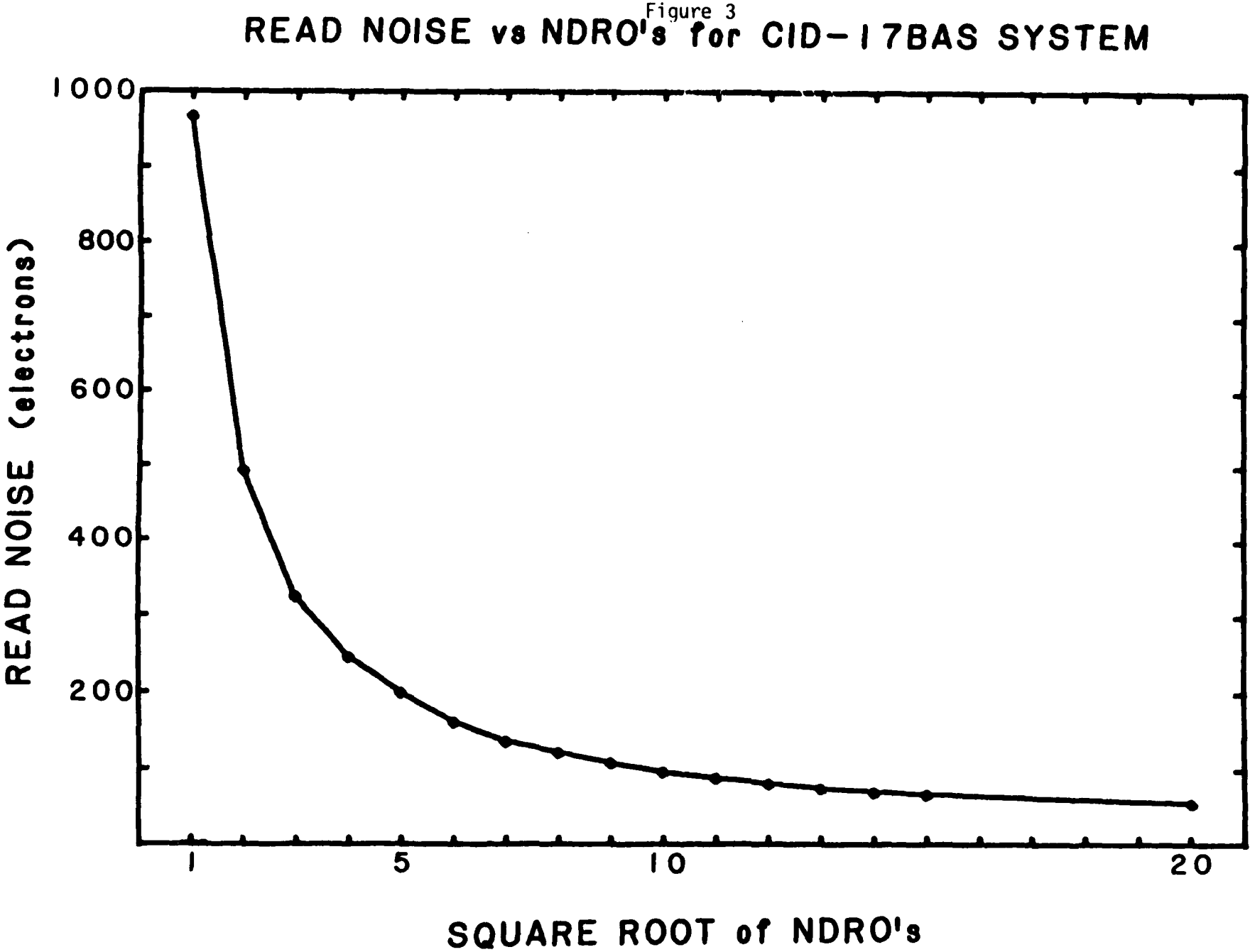
READ NOISE vs NDRO's for CID-17BAS SYSTEM
1000
800
600
400
200
READ NOISE (electrons)
1
5
10
20
SQUARE ROOT of NDRO's

responsivity of the device to shorter wavelength light. Two methods of reducing this effect have been employed in the past. The first is to thin the entire CCD to 10 microns and illuminate the device from the back so that the incoming radiation does not pass through the overlaying gate electrodes on the front of the device [37]. The second method employs virtual phase technology introduced by Texas Instruments [39], in which ion diffusions, instead of polysilicon gates, are used to maintain the required potentials. This greatly minimizes the required number of overlaying gates. While several CCD manufacturers use the thinning process to fabricate backside illuminated CCDs, none of them make thinned backside illuminated linear CCDs. Texas Instruments makes a variety of linear CCDs all of which employ virtual phase technology.

Evaluations of the Texas Instruments TC101 and TC104 have been performed in our laboratory. Currently, there is no commercial source of complete linear CCD detector systems suitable for analytical spectroscopy. As this was the first virtual phase device evaluated in our laboratory, considerable work has gone into the design and construction of the mechanical and electronic systems needed to operate the CCD, including power supplies, camera controllers, computer system, liquid nitrogen cryostat, and temperature controller. After the detector system was functional, significant effort has focused on the optimization and characterization of the electrooptical performance of the system. Even more so than in standard three phase CCDs, it has been found that the selection of the clock voltage levels and timing, to a large extent, determine the performance of the device. Setting the clock voltage levels involves the repetitive process of adjusting the clocks and measuring device performance until optimum conditions are obtained.

The electro-optical properties measured so far in this evaluation include the system read noise, full well capacity, simple dynamic range, blooming characteristics, the characterization of any spurious signals, and the quantum efficiency of the device from 1000 nm to 200 nm. The methodology used for these measurements has been well defined in the evaluation of previous devices, and the test apparatus has been designed and described previously [40,41]. The mean variance method [40] is used to determine the system read noise, the system gain (in electrons/ADU) and the full well. Using this test, the read noise was determined to be 150 electrons, and the full well over 475,000 electrons. In addition, the response of the CCD has been plotted versus light level in Figure 4. As can be seen from Figure 4, the response is linear over the entire operating range of the CCD to within 0.2%, with a slight positive curvature. If one uses a simple second order correction, the deviations from the expected response are less than 0.05% and thus the device is well behaved over its entire operating range.

The TI linear CCD exhibits a luminescent spot caused by the on chip preamplifier acting as a light emitting diode. The light emitting diode causes a spurious signal in the first few detector elements, with the spurious signal decreasing as one moves down the device. The intensity of the spurious signal increases with integration time, and thus the spurious signal is a factor which limits the length of integration time. However, the signal can be completely removed without degrading device performance by lowering the voltage applied to the preamplifier FET drain during integration, and then bringing the voltage back up 2 milliseconds before reading out the device. Figure 5 shows the output of the device without this correction for a 1 second integration time, and with this correction for a 100

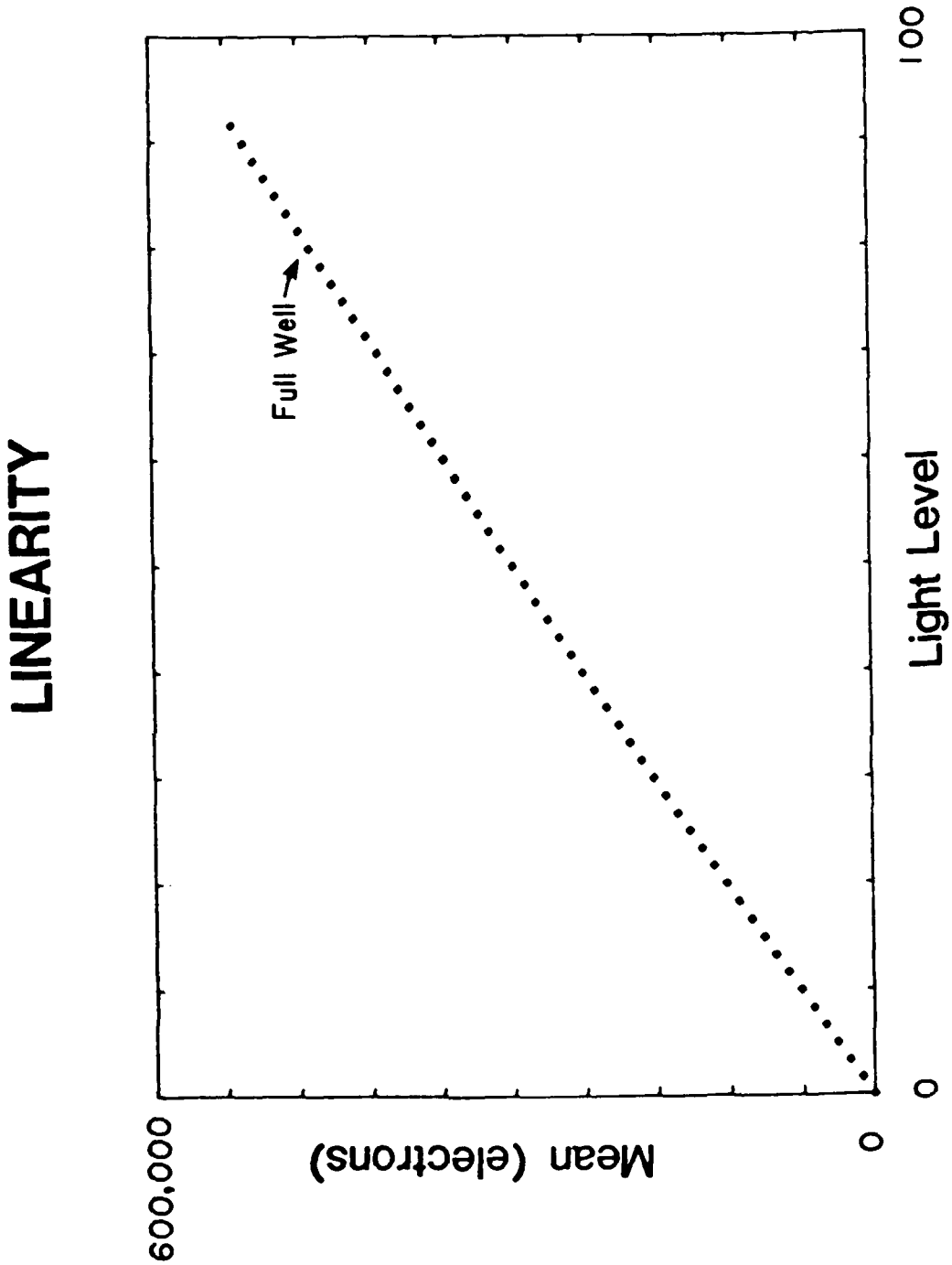

Figure 4
The response of the virtual phase linear CCD to light is a linear function of the illumination level.

Figure 5
The output of the first 300 detector elements of the TI linear CCD for two different operating conditions is shown. The upper trace is for a 1 sec. integration with the drain voltage of the on-chip preamplifier (VDD) set to 25V; the lower trace is for a 100 sec. integration with VDD set to 16 V during integration and reset to 25V 2 msec. prior to readout.

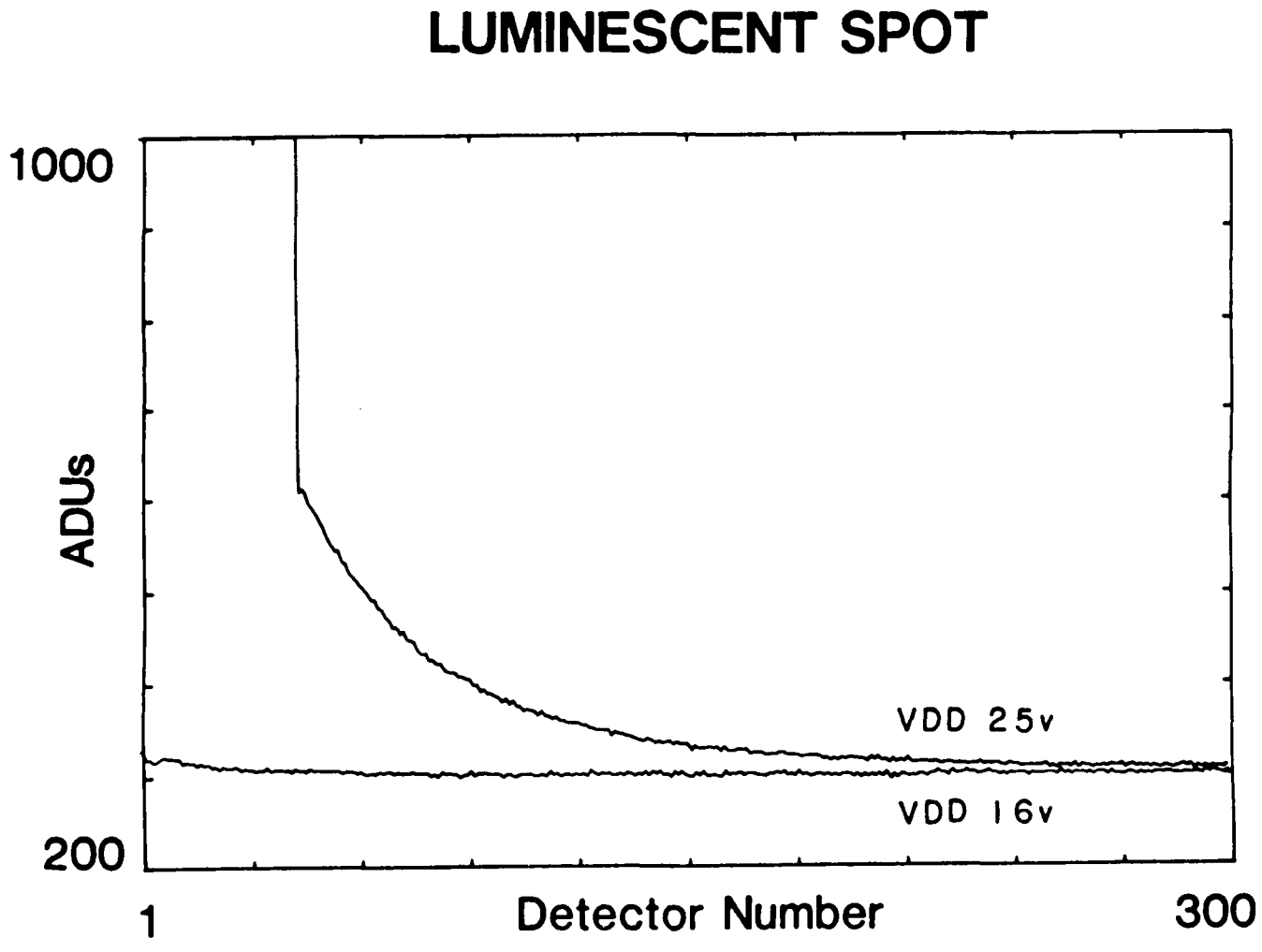

second exposure. As can be seen, no spurious charge can be seen, even with the factor of 100 increase in integration time of the lower trace.

The quantum efficiency of the device has been measured using the integrating sphere spectrometer system, shown in Figure 6. Calibration was performed using a photodiode traceable to the National Bureau of Standards. Figure 7 shows the quantum efficiency of the device from 200-900 nm. The QE of the TI linear CCD is amazingly high, with the QE over 50% from 375-750 nm, and a QE of slightly higher than 100% at 400 nm. One of the features which stands out on this curve is the 105% QE at 400 nm. The definition of QE commonly used in the solid state detector literature is the number of measured electrons per incident photon [35]. The QE can be related to the quantum yield by the equation:

$$QE = QY * QE_1 \qquad (1)$$

where QY is the effective quantum yield with units of number of electrons per interacting photon and QE_1 is the interacting quantum efficiency, with units of the number of interacting photons per incident photon. As the effective quantum yield is not limited to the range of zero to one, but can take on higher values as the energy of the incident photon increases, quantum efficiencies can be greater than one. In fact, it has been reported that the QE of a three phase TI CCD is over 200% for 200 nm photons, and for X-ray photons, QEs over 10,000% are reported [35]. It is important to realize that the TI linear CCD has one of the highest QEs of any solid state detector studied so far over the extended spectral range of 375-800 nm. The oscillations in the QE as a function of wavelength appear to be a characteristic of virtual phase devices, and have been reported in the literature for the evaluation of other two dimensional TI virtual phase devices [35].

Quantum Efficiency Evaluation System

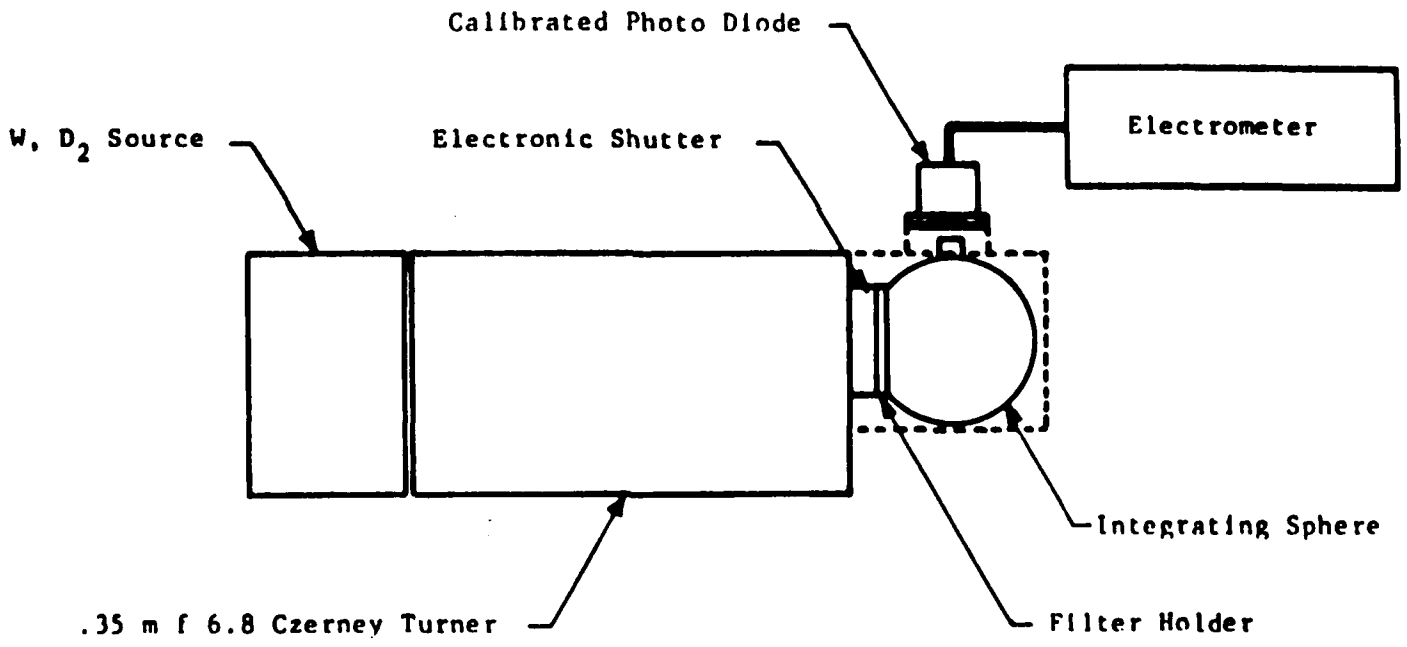

Figure 6
A calibrated photodiode traceable to NBS is used to calibrate the spectrometer prior to quantum efficiency measurements.

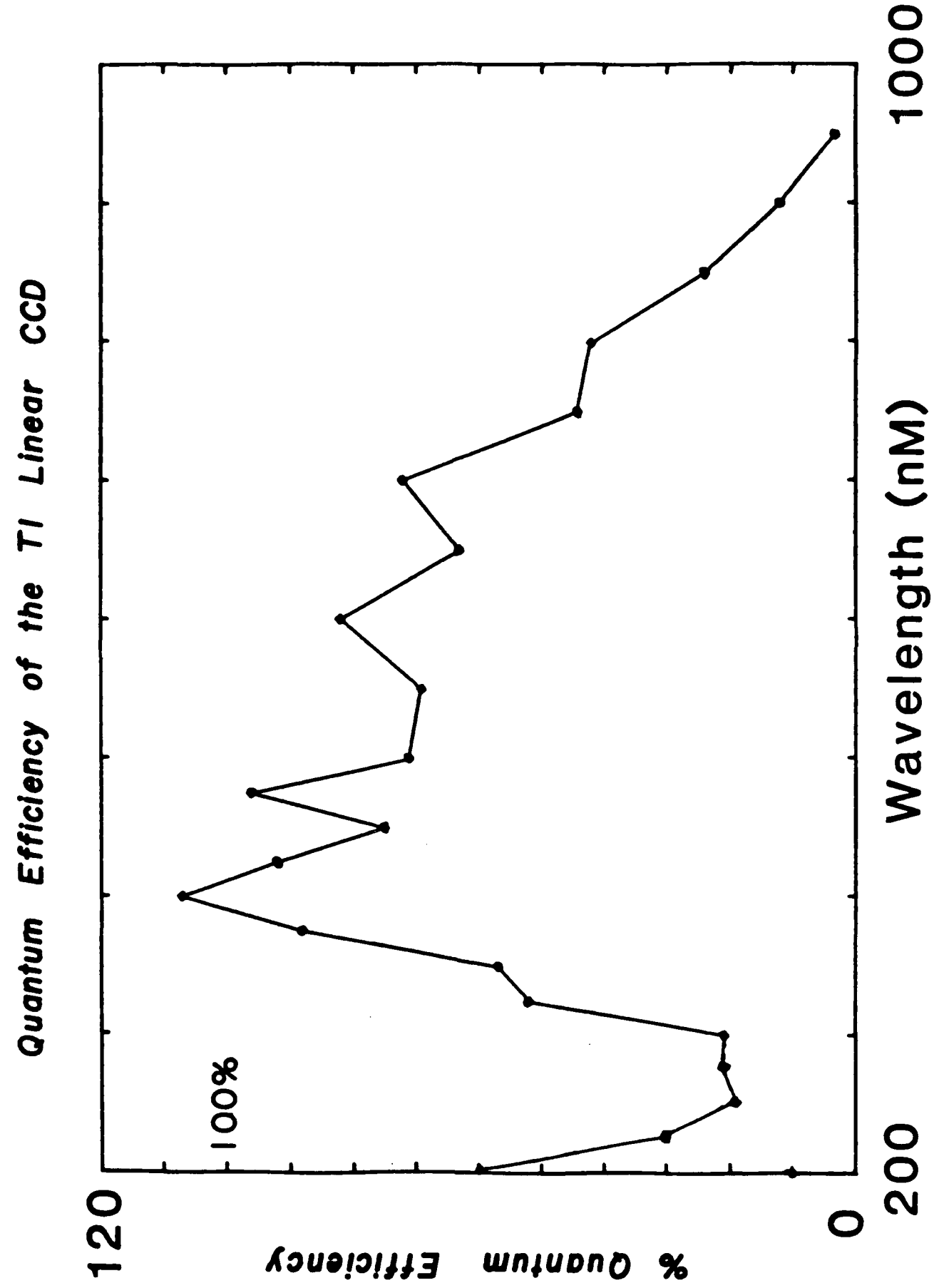
Quantum Efficiency of the TI Linear CCD
% Quantum Efficiency
120
100%
0
200
1000
Wavelength (nM)

Figure 7

During these evaluations, it was observed that the devices do not bloom (spill charge into adjacent photoactive sites) until the full well of the device is exceeded several fold. A possible reason for this can be ascertained by examining the device layout shown in Figures 8 and 9. The CCD consists of a single column of photoactive sites which contain no overlaying gate electrodes. When the device is read, the transfer phase is clocked and the charge collected under the photoactive site is transferred to the transport register, which has been masked with a layer of aluminum to prevent the creation of charge carriers in this part of the CCD. The readout of the device is illustrated in Figure 8. Note that while the CCD consists of a single column of photoactive sites, it contains two transport registers. Charge collected under even numbered detector elements is transferred to the even transport register and charge collected under the odd numbered detector elements is transferred to the odd transport register. To read out the device, the transport phase is clocked, with the charge in both registers being moved down both transport registers one step for each clock. The charge in first the even and then the odd transport registers is sampled in succession by the preamplifier. Because of geometrical considerations, the transport registers have four times the area of the individual photoactive sites, and hence should have several times the charge capacity. When the photoactive site's capacity for holding charge is exceeded, the excess charge appears to spill into the transport register, and hence doesn't cause blooming until the transport register's capacity is exceeded. In fact, this can be used to advantage by simply clocking the transfer phase during integration to transfer the charge collected in the photoactive site into the larger capacity transport register, while the collection of charge continues

Figure 8
Layout of the TC101 CCD showing imaging area, transport registers and demultiplexer. See text for details.

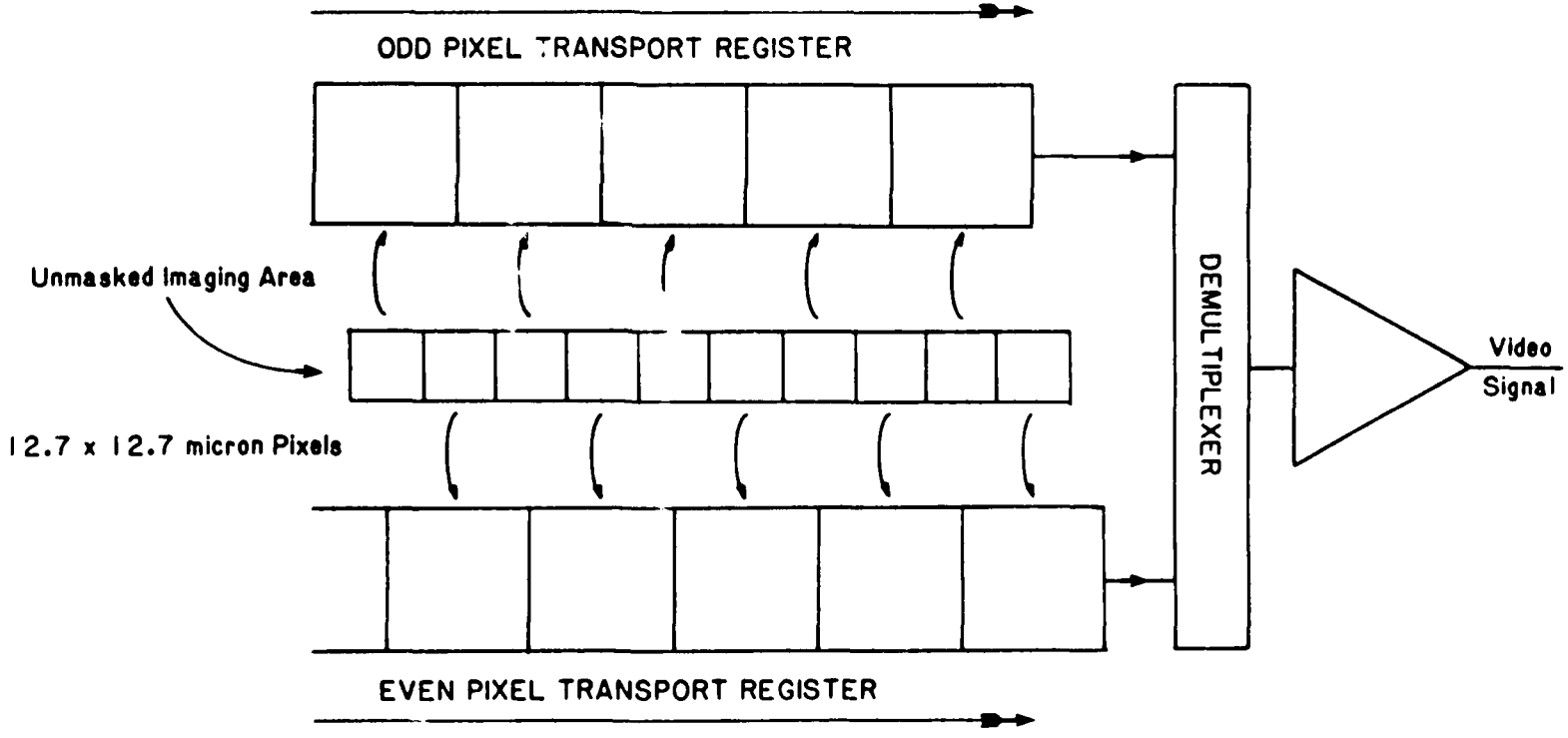

Figure 9

Transfer of Charge from Image Area to Transport Register

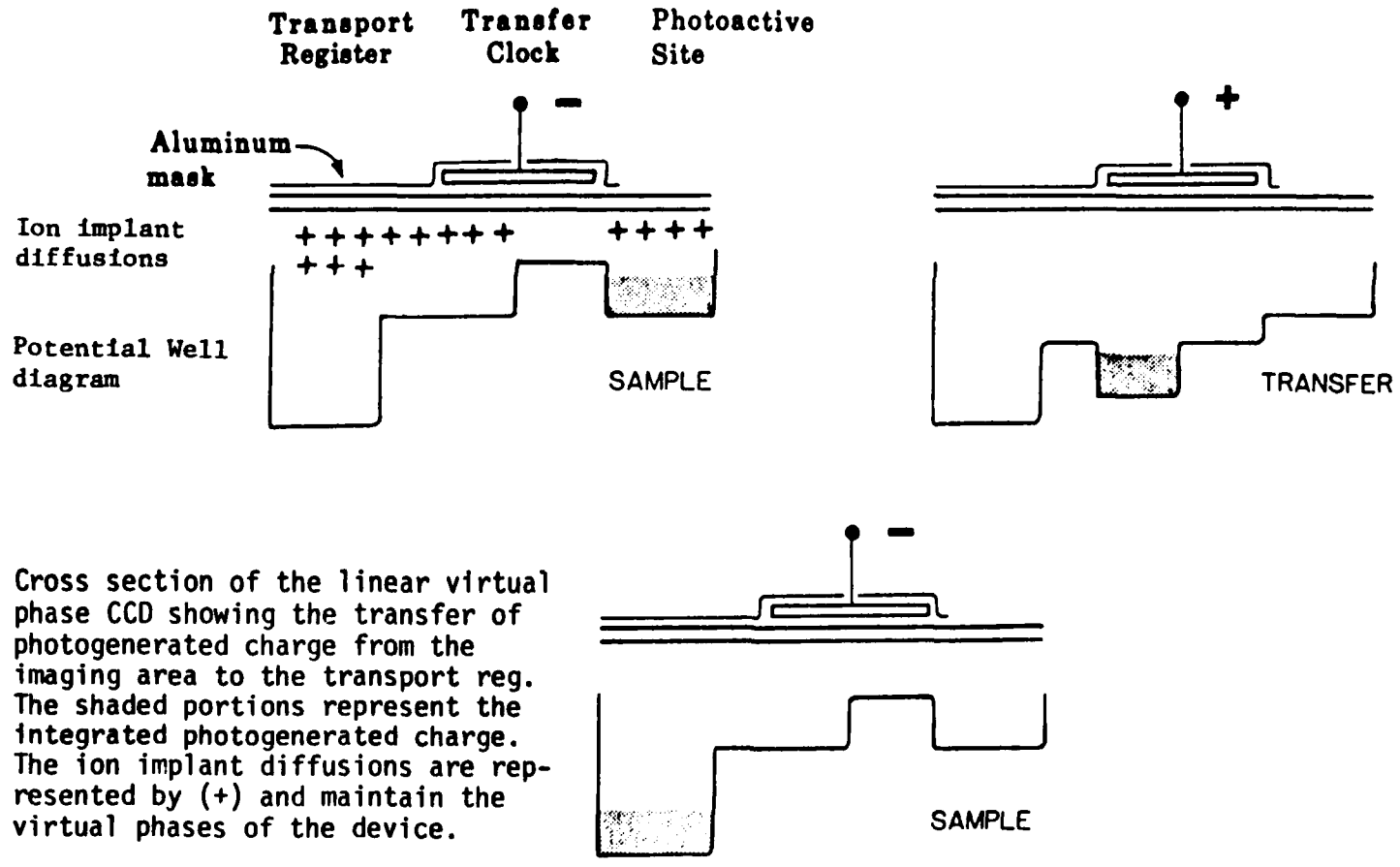

Cross section of the linear virtual phase CCD showing the transfer of photogenerated charge from the imaging area to the transport reg. The shaded portions represent the integrated photogenerated charge. The ion implant diffusions are represented by (+) and maintain the virtual phases of the device.

in the photoactive site. This idea has not yet been tested, and the possibility of spurious charge or extra noise being introduced by the multiple clocking of the transfer phase must be investigated. Currently, the ROM code in the controller and the computer software are being modified to allow this type of charge transfer in the transport registers. This technique could extend the dynamic range of the device by a factor of three or four.

The ability to collect the charge in the photoactive sites and clock them out of the device in a separate set of nonphotoactive registers is unique to this linear CCD. This ability might allow a technique to be used to eliminate the problems caused by blooming. If the transport register is clocked continuously during integration, any charge which overflows a photoactive site will spill over into the transport register and be removed from the device. When one wishes to read out the device, this clocking of the transport register is stopped, and the device is read out in the normal fashion. While this will destroy the information contained in the photoactive site illuminated by the intense spectral feature, it will prevent the charge from the intense feature from blooming and destroying the weak spectral features one is attempting to examine. For this to work, excess charge from the photoactive sites must completely spill into the transport register and not spill into adjacent photoactive sites. Preliminary results confirm this, but changes in the clocking system to allow independent control of both the transfer and transport registers must be made before this can be verified.

The linear CCD detector system performance has been carefully evaluated and optimized and the system has been used in a variety of applications. A UFS-200 Instruments S.A., Inc., spectrograph employing a flat field corrected holographic grating which should give an almost flat focal plane

covering the spectral range from 200-800 nm in a 25 mm focal plane and a miniature gradient wavelength filter have been investigated.

Another application of this linear CCD which has been investigated is the use of the CCD as the detector for a holographic common path interferometric spectrometer. Conventional Michelson interferometers require a mirror which is moved with very high precision, thus resulting in large, mechanically complex interferometers. A holographic interferometer can be used to construct a distinct type of Fourier transform spectrometer which requires no moving parts [42]. This type of interferometer has many advantages when compared to conventional spectrometers. These advantages include the extremely high optical throughput of the system (which is actually higher than the conventional Michelson interferometers) [43] and an inexpensive, stable optical system with no moving parts and no dispersive elements. It is important to note that unlike a Michelson, the interferogram is resolved spatially rather than in time. Thus, the entire interferogram is obtained at a given time, and hence, this technique holds promise for the acquisition of spectral data rapidly, as required for an HPLC detector or for time resolved spectroscopy.

As mentioned above, there are several inherent advantages of using CCDs as the detector for a common path interferometer. In this system, as with conventional spectroscopy, the resolution is ultimately determined by the number of detector elements present. As previously mentioned, CCDs are available in a wide variety of formats including the 3456 element linear CCD, up to the extremely large, 4098 x 4096 element Ford CCD.

Currently, the echelle spectrometer is the only spectrometer system which takes advantage of such a large number of detector elements in a square format. However, the use of a cross dispersing prism or grating in

combination with a common path interferometer offers unparalleled throughput, resolution, and speed for a UV-Vis instrument.

A low dispersive grating has been used to disperse the light in the y direction (see Figure 10), and then be dispersed in the x direction using the holographic interferometer. As an example, let us consider the 2048 x 2048 Tek CCD. For this device, the output of the system would be 2048 separate 2048 point interferograms, each of which contains a slightly different wavelength range of light. For example, interferogram 1014 might contain light from 4040 Å to 4044 Å, and 1015 light from 4044 Å to 4048 Å. The small wavelength range and the boundary conditions forced on the FFT allow high resolution spectra to be obtained for each segment [44]. Note that in this example, to a first approximation, the spectrometer is capable of achieving the incredible resolution of 0.0004 nm with a spectral coverage from 200-1000 nm simultaneously. Using the Maximum Entropy Method (MEM) spectral enhancement technique described below, the apparent resolution can be increased by a factor of 4. This technique has been demonstrated with UV-Vis spectroscopy using a holographic interferometer and a PDA [45]. In addition, the cross dispersion of the light, which separates the spectra into a series of smaller pieces has been shown to greatly minimize one of the larger problems associated with Fourier transform UV-Vis spectrometry -- shot noise. In Fourier transform UV-Vis spectrometry, the shot noise of the entire spectra is spread throughout the spectra (in other words, the shot noise of the centerburst of the interferogram is more or less evenly spread to all spectral features). In addition, the requirement of sampling the centerburst and the weak fringes imposes an incredible dynamic range requirement on the detector. However, spreading the centerburst out among 2000 separate interferograms greatly reduces both of these problems. Each

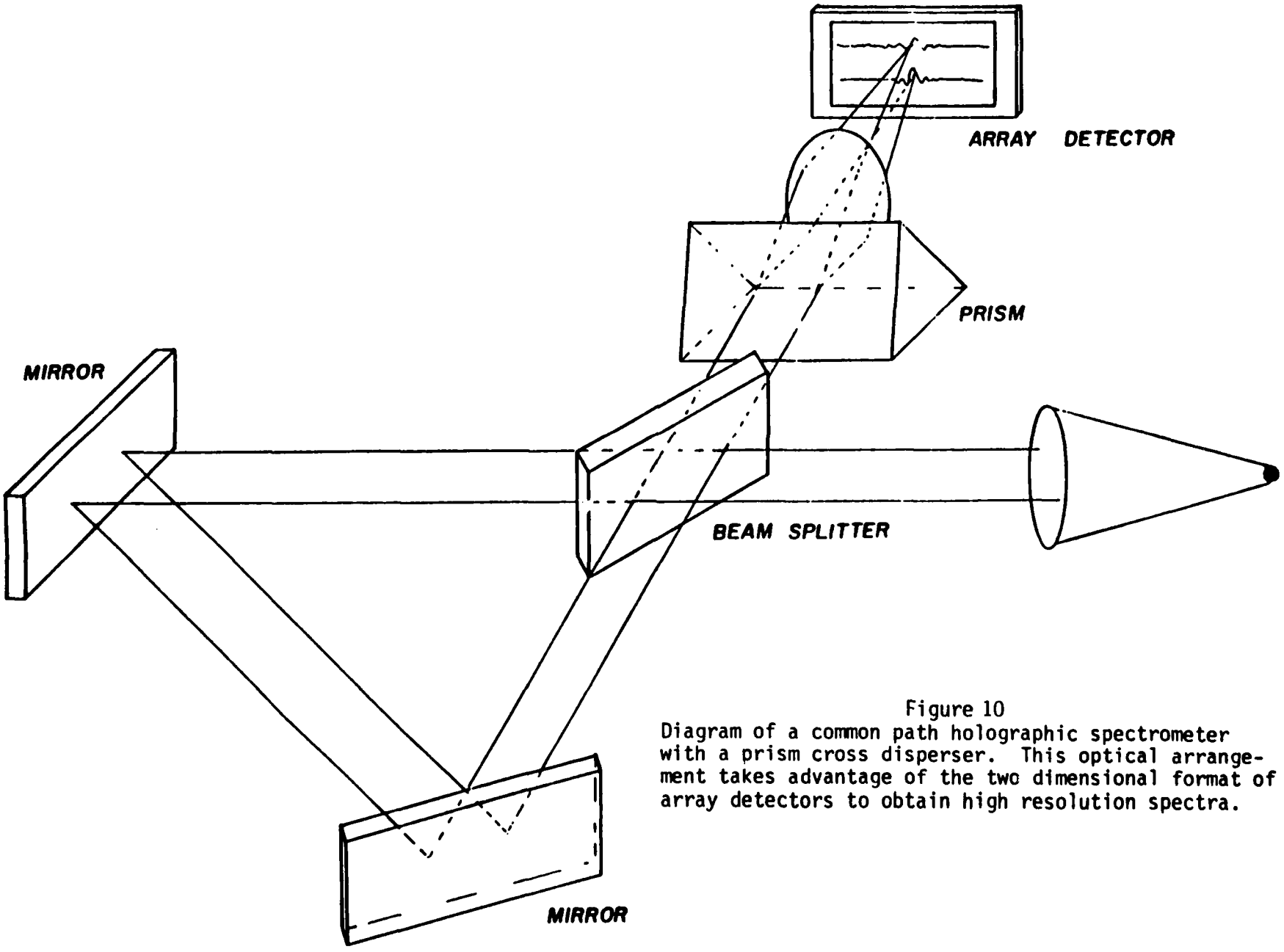

Figure 10
Diagram of a common path holographic spectrometer with a prism cross disperser. This optical arrangement takes advantage of the two dimensional format of array detectors to obtain high resolution spectra.

separate interferogram has its own centerburst and the shot noise in each spectral segment will only interfere with that segment. Thus, this spectrometer system offers unparalleled throughput and performance and is ideal for applications such as continuum AA described in a later section.

The construction of such a spectrometer presented a number of practical problems. Among these are extremely precise mirror and beamsplitter positioning and stability. The design of the computer system and software necessary to perform the thousands of Fourier transforms, in real time, for each spectra is not a trivial matter. As a preliminary study to determine the feasibility of such a spectrometer system, a holographic interferometer system consisting of a beamsplitter, two mirrors, two lenses and several adjustable mounts was constructed. This system initially used the 3456 element TC104 linear CCD. The TI CCD offers several advantages over PDAs for this study. Its antiblooming capability, lack of dark current and its ability to measure small photon fluxes will allow multiple exposures to be performed with varying integration times to increase the effective dynamic range of the detector. The high throughput and high detectivity of the combined FT-UV-Vis CCD system make it an ideal system for applications requiring fast measurements such as HPLC using microbore columns.

The use of the gradient interference filter described previously to limit the spectral bandpass of the FFT-UV-Vis CCD system was explored. The input to the holographic interferometer can be limited to a 10 nm bandpass using the gradient wavelength filter, and then a high resolution spectra of the 10 nm region can be obtained (to a resolution of 0.003 nm). The exact wavelength cutoff of the input to the interferometer, which is determined by the filter position, can easily be determined by taking a low resolution FFT using a white light source. Using the bandpass just calculated, a high

resolution spectra can be obtained. This system allows one to acquire a high resolution spectra over a 10 nm spectral region simultaneously, and then scan the location of this 10 nm window by changing the filter position. The current gradient filter has a range from 300 nm to 750, but one can be obtained with a greater wavelength coverage. This type of simple, low cost system has many applications in its own right, and is a preliminary study to determine the feasibility of building the 2048 x 2048 system described above.

The use of a holographic interferometer allows one to make a simple, low cost, high resolution, extremely high throughput spectrometer. The use of a cross dispersive element, whether a prism, grating or gradient filter, allows one to take advantage of the extremely large numbers of resolution elements available in current CCDs.

Evaluation of Low Noise High QE CCDs for Luminescence Spectroscopy

As mentioned earlier, scientific quality CCDs are the lowest noise solid state array detectors available, making these devices especially attractive as multiwavelength integrating detectors for weak phosphorescent and fluorescent signals. In order to determine the best CCD devices and their optimum operating conditions for low light level spectroscopy, an evaluation program for CCDs has been established. For CCDs to be suitable for luminescence, Raman, time-resolved, or any other spectroscopic application which is photon limited, several criteria must be satisfied. These include low readout noise (typically below 50 electrons), high quantum efficiency throughout the 200 to 1000 nm spectral region, low dark current, and freedom from charge transfer problems.

Linear Spectrograph Detector with Two Dimensional CCD

We have investigated the use of a two-dimensional CCD as a pseudo-linear detector by employing a technique called "binning." Binning is a readout mode of a CCD where charge from more than one detector element is combined on chip before being readout. In the pseudo-linear mode of operation, charge from every element in a column is summed in the serial register, which has the effect of combining 30 by 30 micron detector elements into one large "super element' which could be as tall as 15 mm high. This tall "super element" more closely matches the typical slit height of conventional spectrographs without the use of any reduction optics. Since the charge capacity of the serial register is much greater than the charge capacity of detector elements in the imaging portion of the CCD, binning also increases the dynamic range of the CCD, albeit at the loss of spatial resolution in one dimension. It is important to note that the CCD is the only device where binning is possible and the advantage of summing the analog signal on chip as opposed to summing digital data in memory is that the summed charge is subjected to only one read operation and thus has only the noise associated with one read, whereas the digitally summed data is also summing the read noises from each element in quadrature. If the dominant source of noise is read noise from the detector, then summing in memory will be noisier by a factor equal to the square root of the number of summed elements. Binning can be considered as a way of dynamically altering the "grain size" of the solid state "photographic emulsion" and correspondingly altering the "photographic speed" of the device. We have continued working in accurately measuring noise and the charge capacity of both the imaging array and serial register of CCDs in order to determine the useful dynamic range of each detector. This in turn resulted in a spectrometer

where the dynamic range and the wavelength resolution were traded off against each other depending on the needs of the experiment.

Time Resolved Spectroscopy using a CCD in a Spectral Framing Mode

A unique new readout mode of a CCD has been developed which has been demonstrated to be suitable for time resolved spectroscopy [21] in the microsecond and longer time domain. This mode of operation is termed spectral framing and allows the acquisition of as many as 512 discrete spectra acquired as rapidly as every 2 microseconds. Each spectra contains 320 points and unlike scanning systems, each wavelength is integrated during the entire frame time. Spectral framing mode of operation is illustrated in Figure 11. A spectral image is focused onto the last row of the image region of the CCD. Photogenerated charge is collected in this row during the integration period which corresponds to the spectrum during a frame time. At the end of the integration period the photogenerated charge in each row of the image array is shifted towards the serial register by one row. A new spectral image is then acquired in this last row and the process of collecting and shifting spectral images is continued until the experiment is finished or the image array of 512 rows is filled entirely with spectral images. The charge in the CCD is then read and the complete time resolved spectra is obtained. Each row corresponds to a spectra acquired in a unique time interval while each column describes the time evolution of the light at one wavelength. Figure 12 is the time resolved spectra of a xenon flash lamp over 900 microseconds. The acquisition of spectra is controlled by the clocking of charge in the image array and can be as short as 2 microseconds to as long as minutes or even hours. The time base is computer controlled and can be linear or nonlinear depending on the time dependence of the

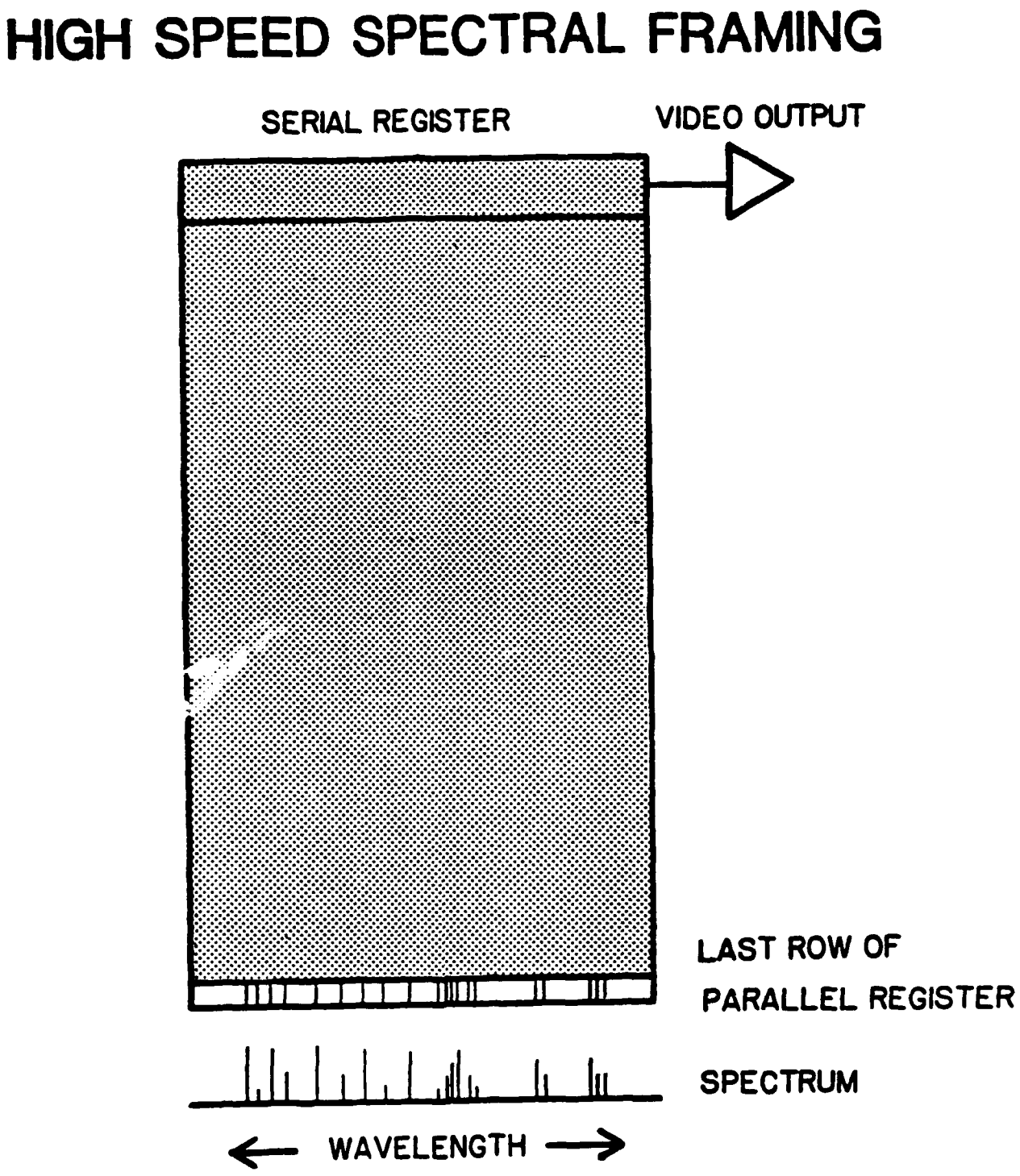

Figure 11
Diagram of CCD used in a Spectral Framing Mode of operation for time resolved spectroscopy.

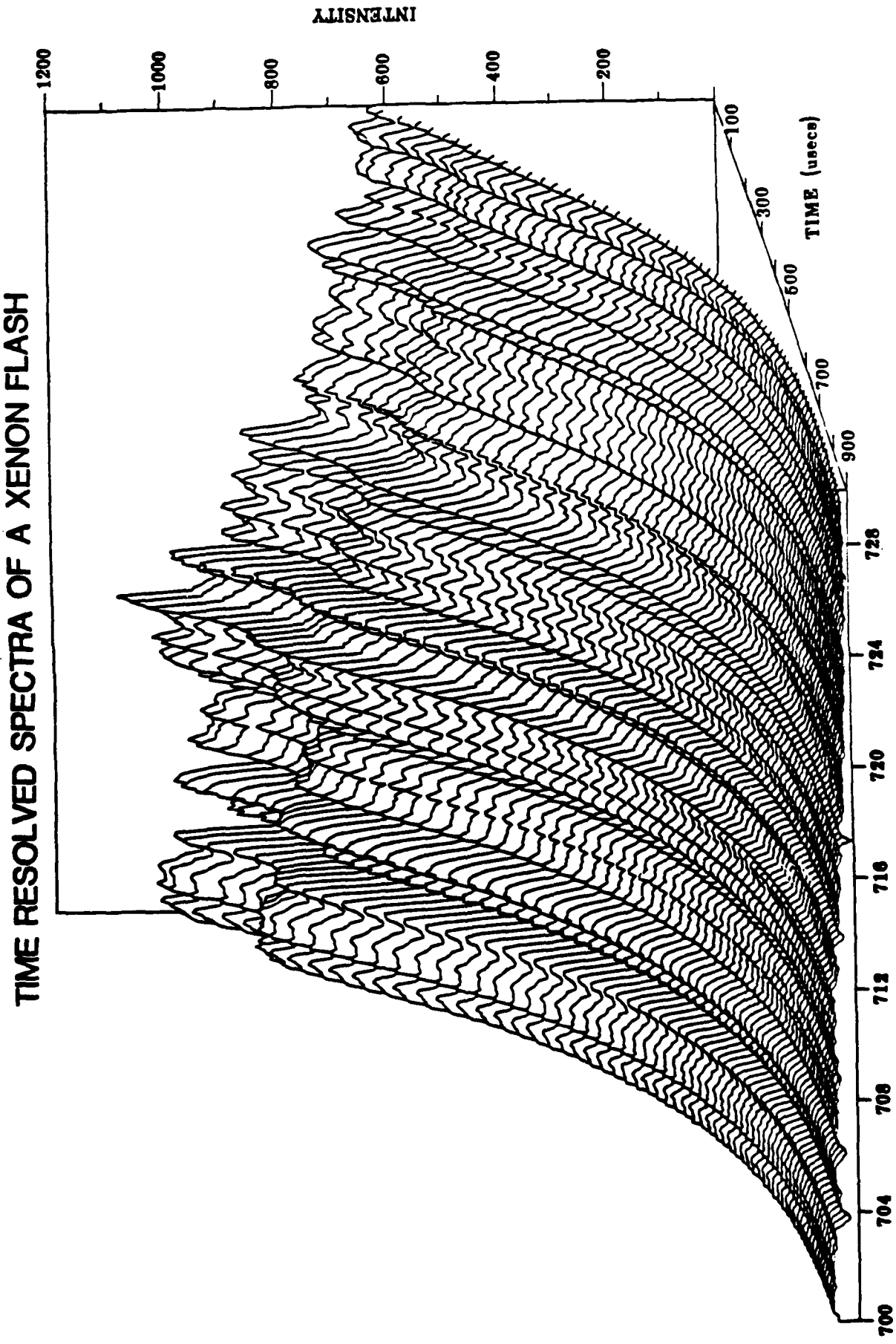

Figure 12
The time resolved emission spectra of a xenon flash over 900 microseconds acquired with a spectral framing CCD.

signal. The 2 microsecond time resolution places this method between mechanical rotating grating rapid scanning instruments which are limited to time resolution of a millisecond or longer, and streak tubes which can have a time resolution of a few picoseconds. The advantage over both systems is the sensitivity of the device for measuring weak transient events without having to average several events. An advantage over streak tubes which achieve time resolution by accelerating and deflecting in time photoelectrons ejected from one photocathode onto a second photocathode, is that charge from each wavelength is integrated in the same detector element during the entire experiment. In addition, in spectral framing photogenerated charge corresponding to a certain wavelength must undergo exactly the same transfer and readout process regardless of whether it was formed early on in the experiment or at the end, thus improving the precision and accuracy of the time base of the measurement. This time resolved spectrometer is rugged, compact, has no moving parts, requires no voltages greater than 20 volts, and is extremely sensitive compared to a single channel scanning system.

Evaluation of New CCDs

Our program of evaluating CCDs is well established and together with Photometrics Ltd. we have evaluated many unique devices from several CCD manufacturers for use in luminescence spectroscopy. In the process of evaluating CCDs for our own use, we have also provided CCD manufacturers with valuable information about the characteristics of their devices.

General Characteristics of CCD Operation

Several phenomena associated with the operation of CCDs can affect their performance in the detection of low light level signals. One phenomenon observed with several detectors during long integrations is light emission from the drain of the on chip FET preamplifier. For normal operation, the output drain, OD, is held at comparatively high voltages of 20 volts or more. This high voltage can cause an avalanche breakdown and impact ionization with subsequent photoemission during hole electron recombination [35]. The result is that detector elements in the corner nearest the preamplifier become saturated with charge during long integration periods destroying any information in this section of the CCD. By lowering the voltages of the preamplifier during long integration periods and then restoring them 50 milliseconds prior to reading of the CCD, we have reduce this self-generated emission by a factor of more than 100. Without this reduction of charge, long integrations of extremely weak luminescent signals would be impossible.

One of the main disadvantages of CCDs compared to CIDs has been the problem of charge spilling from one detector element to adjacent elements upon saturation, a process called blooming. This problem limits the use of the CCD in wide dynamic light conditions, such as might be found when measuring weak phosphorescence in the presence of a strong fluorescent signal. We are studying the problem of blooming in order to determine how it will affect the use of the CCD to record spectral data of a wide dynamic range. A typical CCD with 30 micron square pixels can integrate a total of 400,000 electrons in one detector element before the onset of blooming. Blooming sets the upper limit of dynamic range and can cause loss of spectral resolution. Figures 13, 14,and 15 show the dynamic behavior of

blooming by plotting the intensity of the image from a 25 micron pinhole illuminated with 500 nm light with a 50 mm focal length quartz lens. Figure 13 is an image where the brightest element is at 98% of saturation. Figure 14 is at 117% saturation and charge from the brightest detector element has spilled over into the next element in the same column. Figure 15 shows the image at 350% saturation and blooming is quite evident as charge has spilled over into several adjacent elements along one column. Note that blooming occurs only along columns and not along rows. This mode of blooming can be exploited to increase the dynamic range of our CCD when used as a linear detector for molecular emission spectroscopy. By dispersing spectral lines across the CCD so that the lines run parallel to the CCD columns, any blooming which occurs will not alter the intensity of adjacent wavelengths. This effect could also be used with two dimensional echelle spectrometers by orienting the CCD such that blooming is allowed to spill charge into the dark spaces separating orders and not in the direction of the order.

Future CCD characterization work will expand on devices we are currently familiar with as well as evaluate new prototype CCDs as they become available. Quantum efficiency measurements will be extended into the vacuum ultraviolet for both thinned backside illuminated and virtual phase devices. Fundamental studies of charge transfer effects at low light levels using X-ray sources [35,46] will be performed to determine the CCDs ability to quantitatively transfer charge throughout the device. Several new CCDs with special diffusions implanted in the imaging region of the device will be evaluated with respect to their ability to resist blooming at photon levels past saturation. If these devices are truly nonblooming, they will provide an alternative to CID detectors for atomic emission spectroscopy.

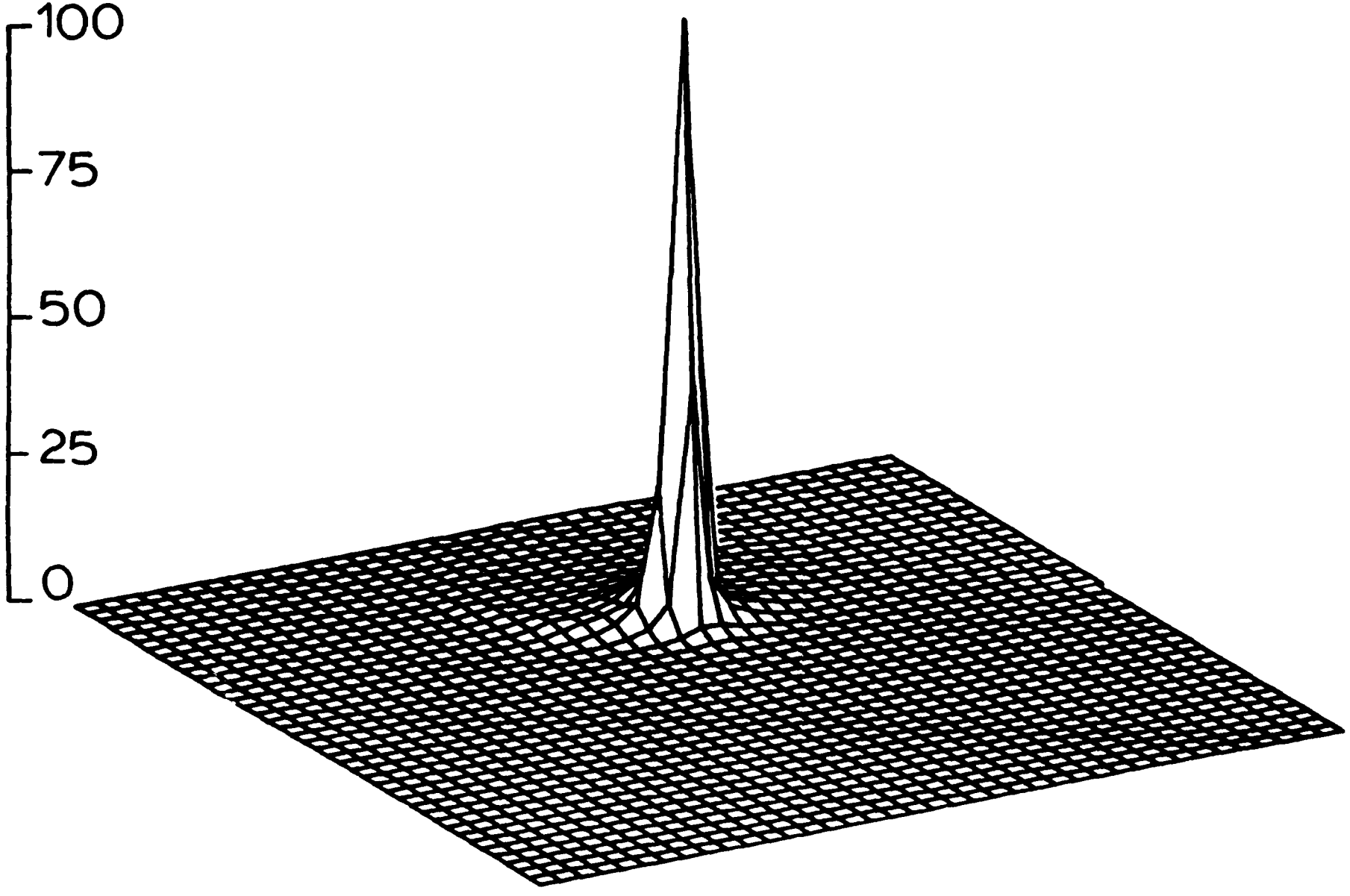

Figure 13
Photogenerated charge from the image of a 25 micron pinhole focused onto the CCD plotted as a percentage of charge full well capacity. The peak of this image is at 98% of saturation.

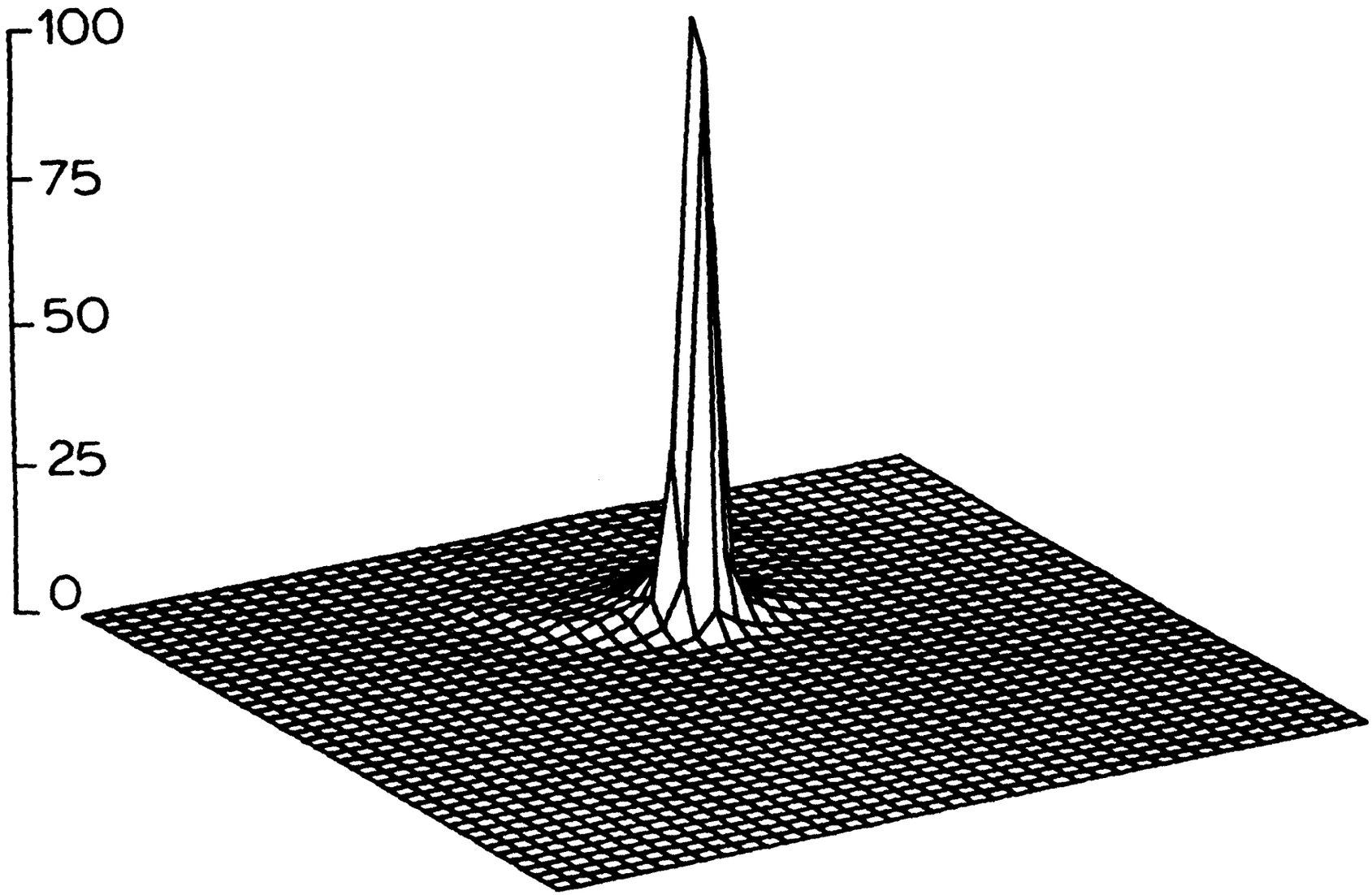

Figure 14
Photogenerated charge from the image of a 25 micron pinhole at 117% of detector element saturation. Note that charge from the peak has bloomed into the adjacent element.

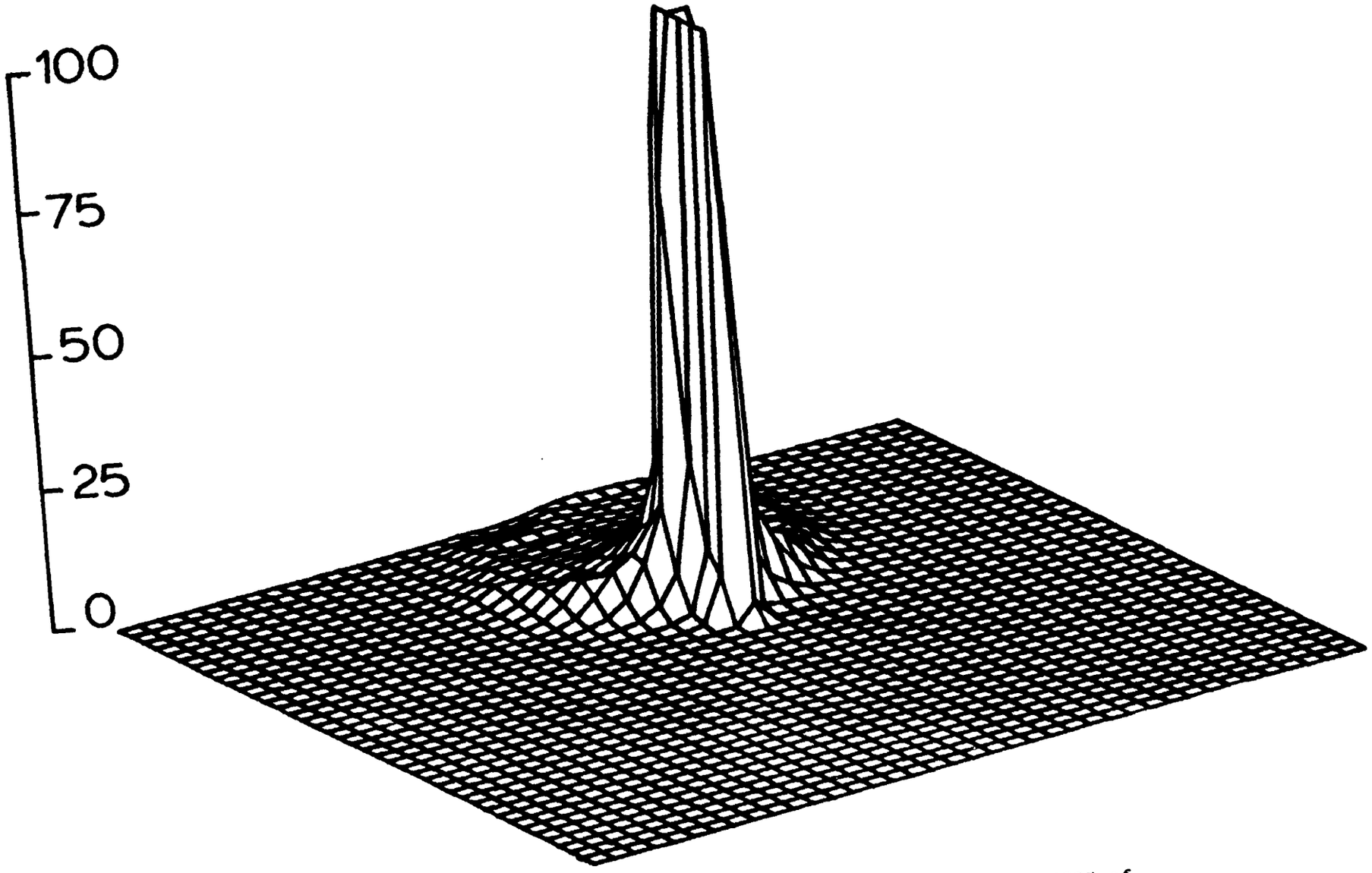

Figure 15
Photogenerated charge from the image of a 25 micron pinhole at 350% of detector element saturation. Note that charge from peak has bloomed into several detector elements along one column.

The benefits of simultaneous multielement analysis, simultaneous background correction and rapid qualitative analysis have prompted many investigations into the application of TV type multichannel detectors to atomic absorption, atomic fluorescence and atomic emission spectroscopy. The more recent attempts have involved the use of silicon vidicons and photodiode arrays (PDAs) in various intensified and unintensified configurations to replace the photomultiplier tubes and/or photographic film found at the focal plane of conventional scanning and direct reading spectrometers. These approaches have met with some success, however, advantages in simultaneity are accompanied by losses in sensitivity and other difficulties such as insufficient dynamic range in the case of vidicons, and insufficient number of resolution elements in the case of photodiode arrays. The problems are particularly severe in the case of atomic emission spectroscopy (AES) where spectral line intensities can vary over five or more orders of magnitude and where high resolution coverage of a wide wavelength range is necessary.

The charge injection device (CID) offers several unique characteristics which help it overcome the problems of sensitivity and dynamic range which have plagued the application of imaging detectors to AES. Additionally, the CID offers several other benefits which are inherent to solid state semiconductor devices such as very high geometric accuracy, ruggedness, low power consumption and resistance to damage caused by light overloads.

The CID-11B was the first device to be incorporated into an entire polychromatic spectroscopy system. The particular CID being used in this series of studies is a General Electric Co. CID-11B, which contains 244 rows and 248 columns of individual detector elements (pixels) for a total of 60,512 pixels. Each pixel is 47 μm long by 35 μm wide, and the overall size

of the photoactive area of this device is 1.1 cm by 0.85 cm. Much knowledge has been gained through this system about how to build better systems.

The camera system comprises a high speed microprocessor based controller, a remote camera head and a host computer. The remote camera head houses the CID detector, clock drivers, all analog circuits, and analog to digital converters. The CID sensor and charge amplifier are operated in a vacuum where they are cooled via a copper cold finger to about $77^{o}K$ with liquid nitrogen. This cooling eliminates virtually all thermally generated charge thereby making it possible to integrate or store charge on the CID for many hours. In the 8 hour study there was only about 50 ADU's increase per detector element which corresponds to only 6.25 ADU's per hour. This compared to a 12-bit resolution (for full-well capacity) of 4095 ADU's shows that on the average each detector element has a dark current of about 0.15% increase per hour and this is independent of total charge stored in the detector element.

The spectrometer used is a modified Spectrametrics Spectraspan III echelle grating spectrometer with a quartz prism cross disperser. An echelle spectrometer was chosen because of its two dimensional display format. This format allows efficient simultaneous examination of a much wider spectral range than with a linear dispersion spectrometer when a two dimensional television camera type detector is used. Initially the collimating mirror was changed from a 0.75 meter focal length spherical mirror to an off-axis parabolic mirror of the same focal length. Also, the camera mirror was removed and replaced by a Schmidt corrected Cassegrain telescope which was used as an image reducer so that a larger spectral range would fall on the detector. A number of studies were conducted with this system. Eventually though, the spherical aberrations created by the image reducer

could no longer be tolerated. A second configuration was implemented where the image reducer was replaced with a 0.35 meter focal length camera mirror and the CID detector and housing were placed inside the spectrometer housing. This modification improved the image quality of the spectral lines immensely but reduced the free spectral range to about one-fifth of its original size. This tradeoff is acceptable because a spectral window was found where a large number of elements of interest at this time emit spectral lines.

Figure 16 shows a typical working curve for the iron spectral line at 271.9 nm. This curve shows the linear dynamic range of a single spectral line extending over five orders of magnitude in concentration. Table 1 gives the linear dynamic range obtained for six elements using multiple spectral lines along with the published values obtained by Spectrametrics under similar excitation conditions and with their standard PMT bank detection system [47]. This comparison shows that the detection limits for each element measured are either better or at least comparable to those of the stock system, and in every case the linear dynamic range goes above that of the stock instrument.

Quantitative analysis of samples with simple matrices has been demonstrated with this system. A multielement sample, containing Cu, Ca, Cr, Ni, Fe and Pb has been made and analyzed. Working curves for each element were run and then the multiple element sample was analyzed at two different concentrations. The results of this type of analysis are given in Table 2 for NI and Cu. The largest source of error in this system probably arises from the DC plasma. Future experiments will include a comparison of this DC plasma with a commercial inductively coupled plasma made by Plasma

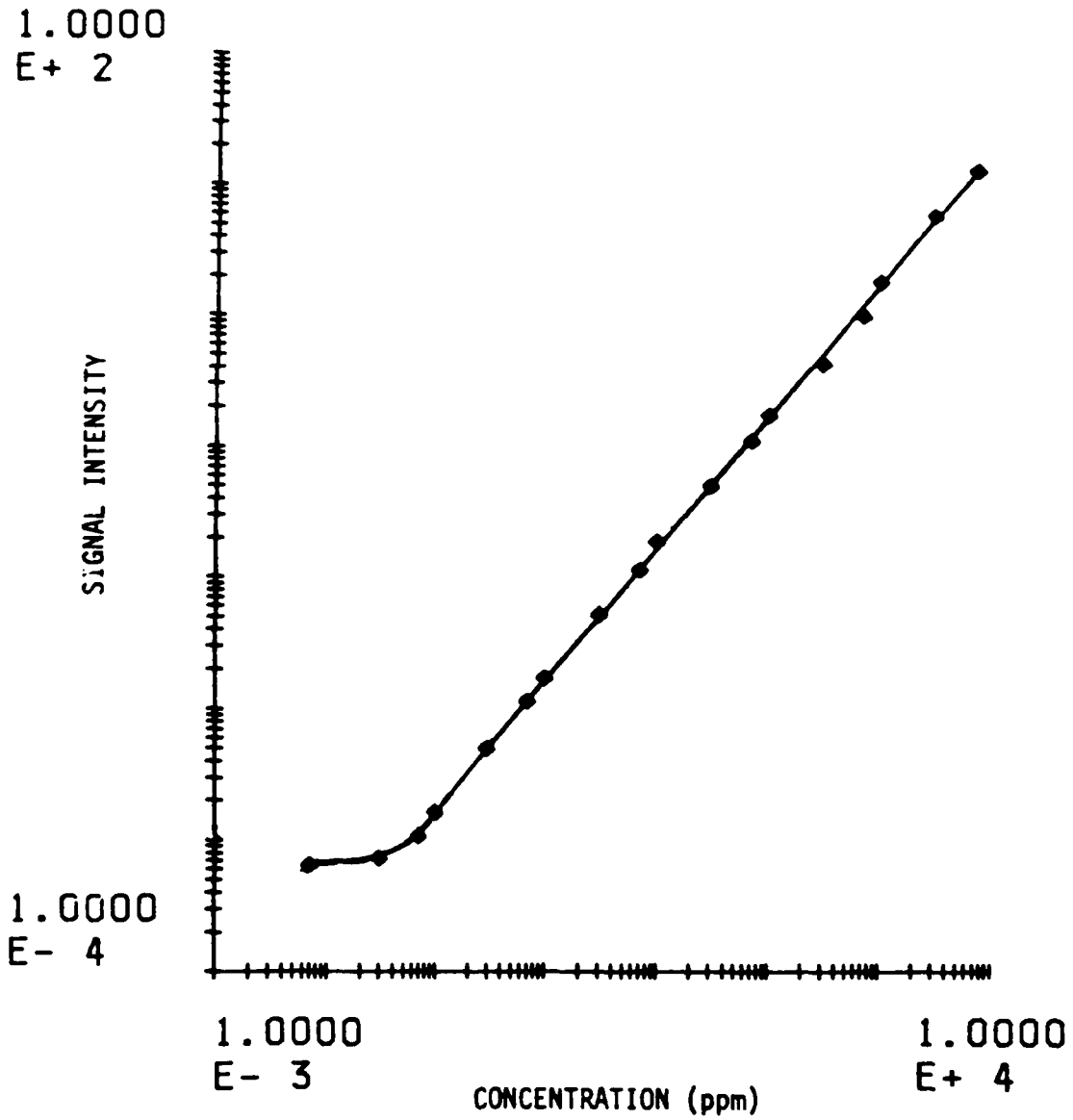

Figure 16
Working curve for Fe at 271.9 nm wavelength

Table 1

Element	Wavelength Detection Limit	Linear Dynamic Range	Spectra Metrics Linear Dynamic Range
Ca	3179Å	<0.001 - 10,000ppm	0.007 - 100 ppm
Cr	3593Å	0.008 - 10,000ppm	0.02 - 1000ppm
Cu	3247Å	<0.001 - 10,000ppm	0.02 - 1000ppm
Fe	2719Å	0.067 - 10,000ppm	0.05 - 1000ppm
Mg	2795Å	0.003 - 10,000ppm	0.002 - 1000ppm
Ni	3619Å	0.02 - 10,000ppm	0.02 - 1000ppm

Table 2

ELEMENT	"TRUE" CONC. (ppm)	MEASURED CONC. (ppm)	REL. ERROR (%)
Ni	30.16 ± .02	30.72 ± .02	1.86%
Ni	80.42 ± .08	78.37 ± .15	-2.55%
Cu	30.02 ± .03	31.91 ± .35	6.30%
Cu	80.04 ± .08	80.78 ± .42	0.92%

Therm Inc. The other possibility is to modify the source to create a more efficient and/or stable excitation source.

The tremendous success of the CID-11 camera/spectrometer system indicates the potential these have for emission spectroscopy. During this period, significant advances have been made by General Electric in CID fabrication technology. These advances have resulted in higher quantum efficiency, lower fixed pattern response and fewer defects. One such "new technology" CID which we have evaluated extensively is the CID-17.

The CID-17 is a 94,672 element array of 23.5 μm by 27.5 μm detector elements arranged in 244 rows each containing 388 detector elements. Characterization of the properties of the device pertinent to spectroscopy as been very nearly completed. The detector responds to light from below 200 nm to over 1000 nm. The response to light is linear to 0.005 percent over a usable dynamic range of over 8000. The dark current of the detector system is less than one charge carrier every two minutes and all photogenerated charge can be removed from the array (injected) in a single inject process requiring less than 10 microseconds.

The effect of the presence of charge at a detector element on the charge measured at a second element is termed crosstalk. Unlike the CID-11, crosstalk in the CID-17 is very slight. The crosstalk occurs to a measurable extent only along columns and is proportional to the total amount of photogenerated charge contained in the column under consideration. The magnitude of the effect is about 0.7 parts per thousand. Because crosstalk is well understood and characterized it can easily be corrected. In spectroscopic applications where a large portion of the array is unlikely to be under intense illumination and hence the total column integrated charge along any one column is not likely to be very large, crosstalk in the CID-17

can usually be neglected. In the case of atomic emission spectroscopy, the first application to which the CID-17 has been put, this has in fact proven to be the case and crosstalk is in almost all analyses ignored. ONR Technical Report 42 [35] describes in detail the characterization of the array detector system.

In light of the improvements made in device operation over the CID-11, and the tremendous success achieved with the CID-11 camera/spectrometer system in simultaneous multielement direct current plasma atomic emission analysis, the construction of a reduced image size echelle spectrometer for the CID-17 camera system was undertaken. It was anticipated that with proper image reduction, true simultaneous multielement analysis could be performed for virtually every element done by conventional plasma emission spectrometry. This is in contrast to the somewhat restricted wavelength region which can be observed by the CID-11 camera/spectrometer system necessitating movement of the prism grating assembly to preselected "windows" where groups of elements may be analyzed.

The ability to mix destructive and nondestructive read modes with CIDs, as first demonstrated with the CID-11 and then with the CID-17, makes them uniquely capable of achieving the very high dynamic range required by modern plasma emission spectroscopy. Our work has shown that the ability to dynamically vary integration time from detector element to detector element while preventing any detector element from saturating allows artificial extension of the linear dynamic range of CIDs almost infinitely. In the two plasma emission systems, dynamic ranges of 7 orders of magnitude are commonly realized. These unique properties make the CID the only multichannel detector capable of meeting the sensitivity and dynamic range requirements of plasma emission spectrometry.

The construction of a spectrometer with a significantly reduced image size was necessary because the optically active area of the CID-17 is only 6.6 mm by 8.4 mm. The instrument is a 750 mm focal length Czerny-Turner system with a Littrow mounted prism cross disperser. An image size reduction of approximately a factor of five is achieved. The spectrometer covers the wavelength range of ≈225 nm to ≈500 nm with .04 to .09 nm resolution. Other properties of the system such as stray light ratios and optical throughput are currently being evaluated. The evaluation is being carried out in two ways. The first method measures the effect of the sacrifices made in optical design in order to achieve a small image in conjunction with the improvements in detection obtained with the use of a CID. This method simply involves the measurement of detection limits for various elements by emission from a commercially available source and comparison to results obtained with conventional optics and PMT detectors. The second method actually involves direct measurement of optical throughput as a function of wavelength and the measurement of stray light.

Mechanical stability of the system is such that removal and replacement of the camera assembly as well as thermal cycling result in no more than a 25 m shift in spectral line positions. This excellent mechanical reproducibility is achieved because the spectrometer contains no moving parts and because kinematic mounting between the camera assembly and the spectrometer is employed. Although this is better than the original design called for, spectral line position shift of even this small magnitude cannot be tolerated.

The original design concept called for active correction for spectral line shift by referencing the emission lines from a mercury pen lamp. A

tremendous advantage of completely solid state detection is that the positions of spectral lines are referenced to the position of some standard so that great mechanical stability and reproducibility is not required. Because of the better than expected mechanical stability of the system however, active correction for spectral line drift is not required. In fact, the stability of the system is so great that if the camera assembly is not removed and replaced, drift in the position of spectral line positions cannot be detected after periods of time as great as several weeks. It should be pointed out that these results are obtained in a laboratory where temperature fluctuations of $5^{o}C$ are quite common and where the only thermal regulation of the system is a small strip heater located near the source region of the spectrometer base.

The only correction for shift in spectral line positions that is performed in the current system is a check for the shift of the mercury 254 nm line using a mercury pen lamp when the camera assembly is removed from the spectrometer. The positions of spectral lines for all elements recorded to date ($\approx$25 elements) are referenced to this line so updating its location effectively updates the location of all of the other lines.

Commercially available echelle spectrometers which use mercury pen lamp emission for wavelength calibration use a more complicated scheme to correct for spectral line position drift. These systems use three mercury emission lines chosen so as to lie at the extremes of the spectrometer field of view. Having three reference points allows for correction of translational errors, rotational errors, and errors involving expansion or contraction (magnification) of the image. Implementation of this type of correction scheme, although not strictly necessary, would enhance reliability of the system and is planned for in the future.

With this system the concept of the "Intelligent Instrument" begins to be realizable. Such an instrument calls on the wealth of information available during the earliest stages of an analysis to decide what parameters and conditions are most suitable for accomplishing the desired analysis.

One of the first steps toward achieving the goal of a truly intelligent spectrometer is the construction of a data base of spectral information from which lines can be selected for an analysis based on the sample at hand. Measurements of dynamic range and sensitivity for each line have been made and stored along with information concerning spectral interferences and potential matrix interferences. Software has been developed to handle the tasks of wavelength selection, background correction, signal acquisition, data reduction, and sample handling. A considerable number of elements have been studied and additional elements are currently under study.

We have demonstrated the unique capabilities of such a system to determine during the early stages of an analysis of a particular sample a number of important characteristics of that sample. Using the method of non-destructive read out, such things as major constituents, background, matrix, etc. of a particular sample could be ascertained during the very early part on the analysis. Based on the data from this preliminary read out, a number of decisions can be made regarding the selection of spectral lines to be used for the analysis. Such factors as approximate concentration of the analyte(s) of interest, presence of spectral interferences, severe continuum, or presence of chemical interferences would dictate whether resonance or ion lines can be selected and which, from a group of possibilities, will offer the most freedom from matrix effects.

Two modes of automatic operation are available. In the first mode of operation, the system queries the operator for the elements to be determined

in advance, and then would proceed automatically to screen the sample for major components and for the approximate concentration of each of the selected elements. Based on the results of this preliminary analysis, spectral lines for each of the requested elements are selected and the analysis performed. This mode of operation employs variable integration time detection at each of the selected wavelengths in order to obtain the maximum signal to noise ratio. In the second mode of operation, a survey of the sample will report to the operator the elements present in abundance and their approximate concentrations. Based on the intensity of a group of lines due to an element, a rough estimate of the elements relative abundance can be made.

The ability to measure a large number of parameters associated with the plasma source continuously throughout an analysis is another very promising and powerful application of this system. With the knowledge of plasma excitation temperature, sample matrix composition, and the concentration of some introduced spike element, a much more accurate semi-quantitative estimate of the concentrations of the components of a sample is possible. Many elemental analysis problems only require a relatively low accuracy estimate of the concentrations of sample components. Considerable time savings results if such analyses are run without the preparation of standard solutions. Sample screening applications come to mind immediately, with only those samples containing a particular element at a level above some threshold receiving accurate quantitative analysis involving the use of standard solutions.

A series of set-up modes of operation will also be available to the analyst. This will allow the analyst with specific goals in mind to override some or all of the automatic line selections, background correction

schemes, etc., and re-educate the spectrometer to perform some specific function.

The potential for built in safeguards in the intelligent spectrometer system is almost unimaginable. On the simplest level, since multiple spectral lines are used for the analysis of each element, checks of self consistency will reveal any unsuspected difficulty with any spectral line. Spectral lines giving results in wide disagreement with others for the same element are subjected to different methods of background correction or disregarded altogether. Checks of this type have been put into practice with the CID-17 camera/spectrometer system and show that the precision of an analysis can be improved as well as its accuracy when the results of determinations using several spectral lines are averaged. Matrix diagnostics are also possible with such a system. In the routine analysis of a series of similar samples, differences in sample matrix that would otherwise go undetected could be called to the operators attention. Differences in sample matrix often require separate sets of standard solutions to be prepared so his type of diagnostic could prevent the reporting of erroneous results. Plasma diagnostics could be performed in a similar manner, detecting unwanted drift in position (particularly DCP), change in temperature (reflecting a change in power or a change in sample matrix), and change in excitation conditions.

Measurement of the ratio of the intensity of a plasma emission line (argon line) to the intensity of continuum in a region of the plasma known to be free from line emission due to the sample would provide a sensitive measure of the change of position of a DCP. This type of relatively long term drift in the DCP, reported to be due to electrode erosion, is a potential source of change in sensitivity. Plasma position must be readjusted or

restandardization must be performed in order to prevent this drift from affecting accuracy. Measurement of the overall intensity of several plasma emission lines at regular intervals would provide an indication of plasma stability. Changes in power or sample matrix would effect these intensities and could also affect analysis accuracy. Changes in the ratios of the intensities of several plasma lines would indicate changes in excitation conditions and would also provide important information to the analyst.

The very excellent quantum efficiency of the CID-17, as shown in Figure 17, points to the potential use of CID detectors in the red and near infrared regions of the spectrum out to 1.1 microns. The curves show that the relative improvements in detection that can be made over PMTs are the greatest in this region of the spectrum. Not shown in this figure is the fact that red sensitive photocathode materials are generally much noisier than blue sensitive materials. This is due to the lower work function materials that must be used to achieve sensitivity to low energy photons. As the photocathode work function decreases, thermionic emission increases, increasing the dark current and hence dark current shot noise. PMTs for low light level applications are usually cooled to minimize thermionic emission, however, PMTs can only be cooled to approximately -20^{o}C before their properties become unpredictable. The dark current in a PMT can never be completely removed by cooling. Unlike PMTs, the read noise associated with an integrating photon detector has no wavelength dependence. The CID-17 detects 800 nm photons with 30% efficiency and 60 electrons of read noise. Because of the inherent noise of red sensitive photomultiplier tubes, the improvements that can be made with CID detection at long wavelengths are even greater than is immediately apparent from Figure 17.

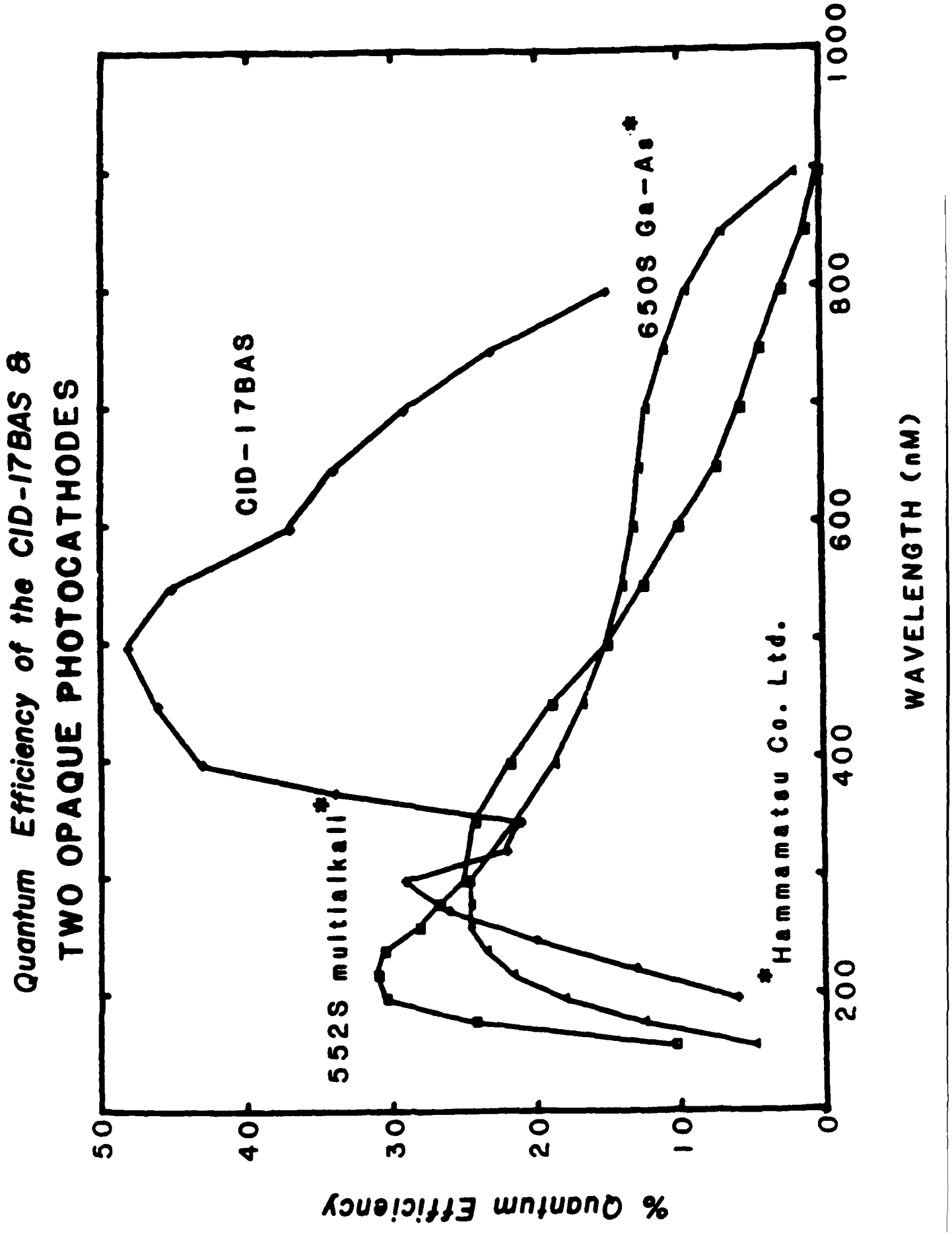
Quantum Efficiency of the CID-17BAS & TWO OPAQUE PHOTOCATHODES
CID-17BAS
650S Ga-As*
552S multialkali*
*Hammamatsu Co. Ltd.
% Quantum Efficiency
WAVELENGTH (nM)
0
10
20
30
40
50
200
400
600
800
1000

Figure 17

A number of researchers are currently investigating the spectral region from 650 to 950 nm as an analytically useful region of the spectrum for nonmetal analysis by plasma emission spectrometry. Although intense resonance transitions for these elements occur in the vacuum ultraviolet, experimental difficulties associated with working in this spectral region have prompted the study of the analytical utility of nonresonance transitions. To date, nonmetal detection limits obtained in the red using ICP and microwave induced plasma (MIP) sources have fallen one or two orders of magnitude short of detection limits obtained in the VUV with ICPs. Although some specialized microwave induced plasma sources operated with helium as a plasma gas show promise for increased sensitivity for nonmetals [48] a great deal of the difficulty with this spectral region may be due to the poor performance of the detectors which have been available.

We have evaluated the spectral region from 600 to 1000 nm for nonmetal quantitative analysis by plasma emission using CID detection. For this investigation we will use existing CID-11 and a microwave source.

He-MIPs have given satisfactory results when used as gas liquid chromatography detectors, however, the direct introduction of sample aerosols can dramatically reduce analyte emission intensity or extinguish the plasma. Our experience with high power ICPs running at altered pressures and with a variety of plasma gases has shown that these plasmas are stable and accept large quantities of sample aerosols in a variety of forms [20]. We have successfully investigated these sources as alternatives to atmospheric pressure argon plasmas for nonmetal analysis.

In most cases, the ultimate sensitivity of the CID plasma emission method depends on the intensity of background emission at the wavelength of analyte emission. Only in cases where background emission is extremely low

is the detection limit determined by other factors (usually source drift). High frequency source flicker is much less significant in determining detection limits when integrating photon detectors are employed as compared to PMTs. This source of noise does not seem to be important in DCP and ICP sources when using CIDs.

In the case where background emission determines the detection limit, detector element saturation level plays a similar role in determining the minimum detectable signal as it does in absorption measurements. In the emission measurement, the subtraction of the background signal (I_b) from the analyte-plus-background signal (I_t) must result in a value greater than zero for the analyte to be detected. Since there is a noise component associated with the measurement of I_b, and also a noise component associated with the measurement of I_t, this difference (I_a) must also be larger than twice the uncertainty that results from the subtraction. As in the case of absorption measurements, maximum signal to noise ratio is obtained when fluxes are allowed to integrate to near device saturation. The rms noise on the signal, being due primarily to shot noise, equals the square root of the signal. A detection limit condition can be defined as:

$$I_{a,min} = 2(\lambda^2(I_t) + \lambda^2(I_t - I_{a,min}))^{1/2} \qquad (2)$$

where $I_{a,min}$ = the minimum detectable signal due to the analyte,

$\lambda(I_t)$ = the uncertainty in the intensity of the signal from the background plus analyte, and

$\lambda(I_t - I_{a,min})$ = the uncertainty in the intensity of the signal from the background (I_b).

As stated above, the principal source of noise is shot noise so:

$$\lambda(I_t) = (I_t)^{1/2} \text{ and,} \qquad (3)$$

$$\lambda(I_t - I_{a,min}) = (I_t - I_{a,min})^{1/2} \qquad (4)$$

Substituting the relations for shot noise in terms of the signal magnitude (3 and 4 above) into equation 2 results in:

$$I_{a,min} = 2(I_t + I_t - I_{a,min})^{1/2} \qquad (5)$$

Solving equation 5 for $I_{a,min}$ results in:

$$\frac{I^2_{a,min}}{8} + \frac{I_{a,min}}{2} - I_t = 0 \qquad (6)$$

The solution of equation 6 is:

$$I_{a,min} = 4(1/4 + I_t/2)^{1/2} - 2 \qquad (7)$$

recognizing that I_t in terms of charge carriers is a large number, $I_{a,min}$ may be approximated as:

$$I_{a,min} = 4(I_t/2)^{1/2} \qquad (8)$$

Detection limits which are limited by background emission may be improved by increasing detector full well capacity until the point where

integration time becomes so long that source drift becomes the limiting factor. Expressing $I_{a,min}$ as a fraction of I_t shows how the sensitivity of an emission measurement made under conditions of background emission limitations improves with device dynamic range.

$$\frac{I_{a,min}}{I_t} = \frac{4}{(2I_t)^{1/2}} \qquad (9)$$

Our investigations of the red and near infrared for quantitative analysis of nonmetals by plasma emission have yielded detection limits dictated by source background emission.

Only in the case where the detection limit is not determined by background emission will improvements in spectrometer throughput or detector sensitivity lead to improvement in detection limit. This is only the case at short wavelengths (below 225 nm) in the current CID-17 camera/-spectrometer system. The instrument currently has a long wavelength cutoff of ≈500 nm, far from where throughput and sensitivity are lacking. Previous discussions of the merits of CCDs and CIDs show the relative improvement of these devices over PMTs and the narrowing gap between currently available technology and "perfect" photon detection. Noting these facts leads one to the conclusion that improvements in detection limits will require improvements in sources and in some cases improvements in spectrometer throughput but that when using CCDs or CIDs detectors are no longer the limiting factor.

ARC AND SPARK SOURCE EMISSION SPECTROSCOPY WITH AN OPTIMIZED ECHELLE–CID SPECTROMETER

The classic techniques of spark source emission spectroscopy also has benefitted from the enhanced capabilities of the CID detection scheme.

The spark source is a well known sensitive technique for direct qualitative and quantitative analysis of solids. In recent years the use of technique for qualitative analysis has lost ground to flame and plasma emission spectroscopy because of the inconvenience of calibrating, developing and reading photographic emulsions and certain inherent problems limiting accurate quantitative analysis.

However, the spark does not require liquid samples, eliminating the major time-consuming task of sample dissolution. This is particularly important when a large number of solid samples are to be screened.

An appropriately configured echelle–CID spectrometer would eliminate the problems associated with photographic emulsions. Traditionally, multielement spark spectroscopy has found greatest application in process and quality control associated with the production of metals. As in the cases of plasma and arc excited emission spectroscopy, use of an optimized CID–echelle system with a spark source should greatly enhance the techniques capabilities.

The very complex nature of spark excited spectra can be more readily dealt with both qualitatively and quantitatively through high speed computer manipulation of the large data base available from the CID-echelle system. No longer is the user always be forced to use only one or two lines per element as is common in alloy analysis. No longer is qualitative analysis almost impossible.

To prove these concepts a National Spectroscopic Laboratories model 6187 combination arc/spark source and source stand has been interfaced with one of our custom CID–echelle spectrometers.

Detection limits, precision and accuracy have been determined using a series of National Institute for Standards and Technologies alloys. While limitations inherently present due to the excitation mode still exist, significant improvements in techniques have been gained through accurate computer processing of the complex spectral data.

Single Pixel Charge Injection Device

Today's CCDs and CIDs offer many advantages which make them very attractive as detectors for spectroscopy. As the previous discussions demonstrate, these devices are the premier detector for low light level applications on a single detector basis, not even allowing for the huge multiplex advantage that they offer. The next logical step is to make a large single element detector to compete directly with photomultiplier tubes for single channel applications. After many years of trying to convince CCD and CID manufactures of this need we have recently been successful. We are currently interacting with the engineering staff at CIDTEC to implement such a detector. Recently we received several of these experimental devices from GE for evaluation. The feedback from our evaluations will allow GE to decide if this device is a viable product.

Before describing the advantages of these new devices, it is important to understand the limitations on current photomultiplier tubes (PMTs). Most analytical spectroscopists still regard the PMT tube detector as state of the art in low light level optical detection. When operated in the photon

counting mode, the PMT has many attributes which have made it the choice detector for nearly every type of low light spectroscopy. Despite its overall good performance and the tremendous success of the PMT, this detector has many limitations which result in it being far from perfect. In addition to the previously discussed limitations encountered when using PMTs including limited spectral range, low QE, and high dark count rates, several other problems exist. Exposing a PMT to typical room light conditions while the detector is operating will destroy it. Select photon counting PMTs are even more sensitive in that exposing these detectors to even moderate light levels will cause a dramatic and usually irreversible increase in dark count rate. This problem occurs even with no power applied to the tube.

These deficiencies point out the need for a superior detection system for extreme low light level applications. The single element charge injection device (SECID) promises to be such a detector. The operating principles of this device are similar to the more conventional charge injection device imaging arrays in that charge is generated and stored in an epitaxial N doped silicon layer by the absorption of photons. The accumulated charge is then measured via an intracell charge transfer process [41]. The unique feature of this readout mechanism is that the charge measurement process is either non-destructive, i.e. the quantity of charge in the sensor is not altered during measurement and can thus be repeatedly determined, or destructive, i.e. the charge is removed.

The sensing area of the experimental SECID is 1 mm^2. This is extremely large when compared to the individual detector elements in CCD and CID array detectors. Because of the large charge sensing and storage area, the charge storage capacity is enormous. We have measured this to be 130 x 10^6

electrons. As with other CCDs and CIDs, the sensor exhibits no permanent adverse effects from prolonged exposure to extreme light overload.

Advanced Sample Introduction Techniques

During the course of this project, considerable progress has been made in developing nebulizers capable of allowing direct analysis of very complex samples. A variety of nebulizer configurations have been evaluated including new Babington geometries optimized of high performance liquid chromatography, blood analysis, etc. and the heated Babington Principle nebulizer for the direct determination of wear metals in lubricating fluids.

The need for rapid, accurate determination of wear metals in lubricating oils has long been documented [49-55]. Such analyses could save significant amounts of money in both military and private applications by providing a profile of the condition and wear of mechanical systems and predicting premature failure and the need to rebuild [55]. Current commonly used methods such as solvent dilution atomic absorption (AA) spectroscopy and inductively coupled plasma atomic emission spectroscopy (ICP-AES) give results which are known to exclude metal present in the form of particulates as the particulates settle out of the diluted oil and are never aspirated into the source [56]. The use of ashed AA does give total metal content, but this method is very time consuming and technician intensive as well as providing ample opportunity for sample contamination.

Data using direct injection of lubricating oils into an inverted ICP have been promising. A sample of oil is drawn directly from the operating engine using a syringe and is injected into the ICP using the same syringe

with a stepper motor controlled sample introduction system. The particulates present in the sample in the inverted ICP system fall through the plasma rather than settling out. Linear working curves have been established over at least two orders of magnitude using a variety of organometallic standards in lubricating oils and results obtained have compared favorably to ashed AA studies [56]. The use of a heated modified Babington principle nebulizer has virtually eliminated the viscosity effects of various weights of motor oil.

Improved Efficiency Nebulizer

Significant gains have been made over the course of this project in reducing the quantity of the sample lost down the Babington principle nebulizer drain. Today "Babington principle" nebulizers bear virtually no resemblance to the hollow sphere pierced by a hole of the original design. However, as with other commercially available nebulizers such as the Bernoulli, crossed capillary, MAC, etc., a sizable amount of sample is lost. In attempts to improve on this situation, several workers have investigated glass frit nebulizers [57-60]. By forcing nebulization gas through the frit while flowing solution over the frit, a high quality aerosol has been reported. Additionally, loss of sample down the nebulizer drain can be drastically reduced.

The frit nebulizer can easily be regarded as a multiple orifice Babington where the number of orifices has been carried to the extreme. Unfortunately, this nebulizer has a rather significant problem with sample carryover or crosstalk. This fact is not totally surprising when one considers the vast number of crevices present in the frit, not all of which are flowing nebulization gas. These "blind alleys" provide sites for a sample

to "hide in" and slowly bleed out of into subsequent samples. We have recently configured a nebulizer which greatly minimize this problem while retaining the high sample efficiency of the frit.

In this nebulizer, a type of capillary array originally developed for microchannel plate image intensifiers is used in place of the frit. These arrays consist of a very large number of relatively precise diameter capillaries fused together into a disc.

Since the technology must accurately reproduce an optical image with good fidelity, blemishes, plugged capillaries, etc., must be minimized. The "blind alleys" and other sites present in the frit are either eliminated or at least greatly minimized. Capillary diameters are available over the size range we consider (based on frit data) most optimal (i.e., 2, 3, 5, 10 μ). Studies conducted in our laboratories and by Jeff Babis at Beckman Instruments indicate high quality aerosol can be produced and sample crosstalk is greatly reduced.

EXCITATION PHENOMENA IN INDUCTIVELY COUPLED PLASMA

Inductively coupled plasmas have been used for qualitative and quantitative analyses for well over a decade, yet many of the fundamental excitation and energy transfer processes are still not fully understood. Lovett [61], Boumans and De Boer [62], Blades and Hieftje [63], and many others have proposed models that explain some of the phenomena occurring within the plasma. However, no one theory advanced so far has proven to be completely successful. A study of rates and reaction mechanisms within an inductively coupled plasma operating at a variety of working pressures promises to prove quite valuable in providing additional insight into the

basic nature of the analytical plasma. The fundamental knowledge gained through the study and characterization of analytical plasmas is providing basic insight into plasmas used for other applications such as plasma etching and glow discharge phenomenon.

Existing literature [64-66] dealing with the use of radio frequency inductively coupled plasmas operating at other than atmospheric pressures has been confined, for the most part, to studies of homogeneous plasmas operated at reduced pressures. These studies establish the basis for pursuing this line of research but are of little value in describing the mechanisms within an analytical inductively coupled plasma. The studies by Medgyesi-Mitschang and Hefferlin [67] demonstrated that operating pressure did effect the emission intensity and therefore the excitation temperature of the plasma support gas.

Plasma Equilibrium

Numerous previous studies [68-73] have demonstrated that Local Thermal Equilibrium (LTE) conditions do not exist within an ICP operating at atmospheric pressure. Local Thermal Equilibrium is a state in which all energy distribution functions with the exception of that of the radiant energy are given by Boltzmann distributions. The departure of atmospheric ICPs from LTE is manifested in the fact that the observed electron densities cannot be reconciled with the spectroscopically measured excitation and ionization temperatures. In fact, the measured excitation temperatures for different species in the plasma are inconsistent. Caughlin and Blades [68] have shown that the experimentally determined ion-atom emission intensity ratios in an atmospheric pressure ICP are less than calculated LTE ion-atom emission intensity ratios. Medgyesi-Mitschang and Hefferlin found that for plasmas

operating at reduced pressures the electron density decreased while for pressures below 300 Torr the Ar atomic emission intensities increased with decreasing pressure. In order to study the effect of torch pressure on the operation of an analytical ICP a variable pressure torch was designed and built (see Figure 18). The system allows the torch pressure to be varied between 100 and 3000 Torr while the plasma is in operation.

Studies performed using the altered pressure torch system have shown the same trends as observed by Medgyesi-Mitschang and Hefferlin for the pressure region below 300 Torr. It was found, however, that the emission intensity and therefore the excitation temperature of the support gas (argon) and analyte species increased with pressure above 300 Torr (Figure 19). Studies investigating analyte excitation temperatures showed no increase with decreasing pressure below 300 Torr (Figure 20), indicating that the excitation mechanisms are such that at lower pressures the interaction between the analyte and the plasma is reduced. Calculations of relative electron densities within the plasma indicate a marked increase in electron density with increasing pressure. The higher the electron density, the more likely the excitation processes in the plasma are collisionally dominated, and therefore the plasma should be closer to local thermal equilibrium (LTE) as defined by Caughlin and Blades [68]. This shift towards LTE is particularly useful because LTE conditions are often assumed, thus allowing use of LTE formulae (such as the Saha equation [74]) for the calculation of ion, atom, and electron distributions within the plasma. Through the manipulation of torch pressure, to adjust plasma conditions closer to or farther away from LTE, the validity of the LTE assumption for atomospheric pressure ICP can now be determined.

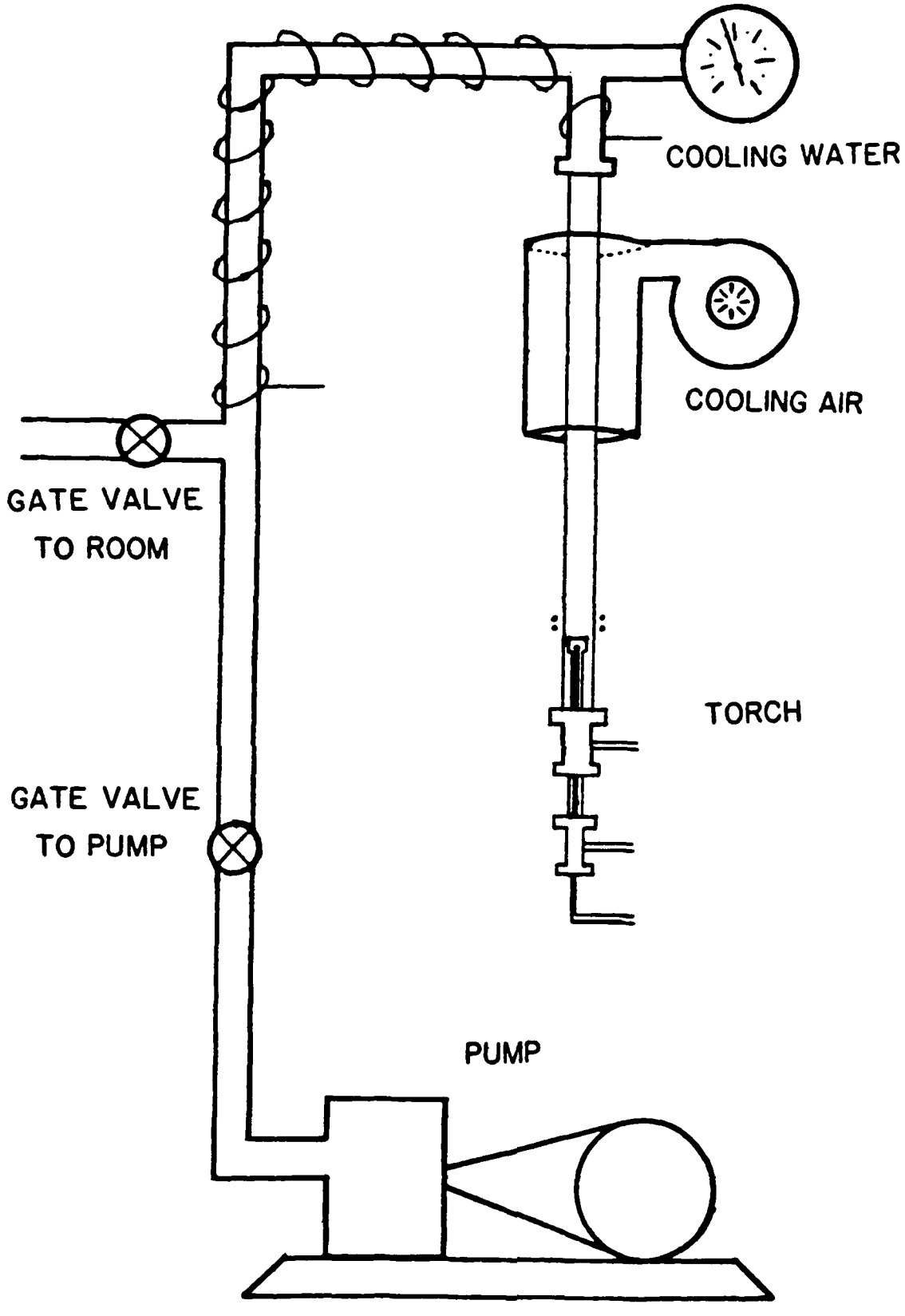

ALTERED PRESSURE TORCH SYSTEM

Figure 18

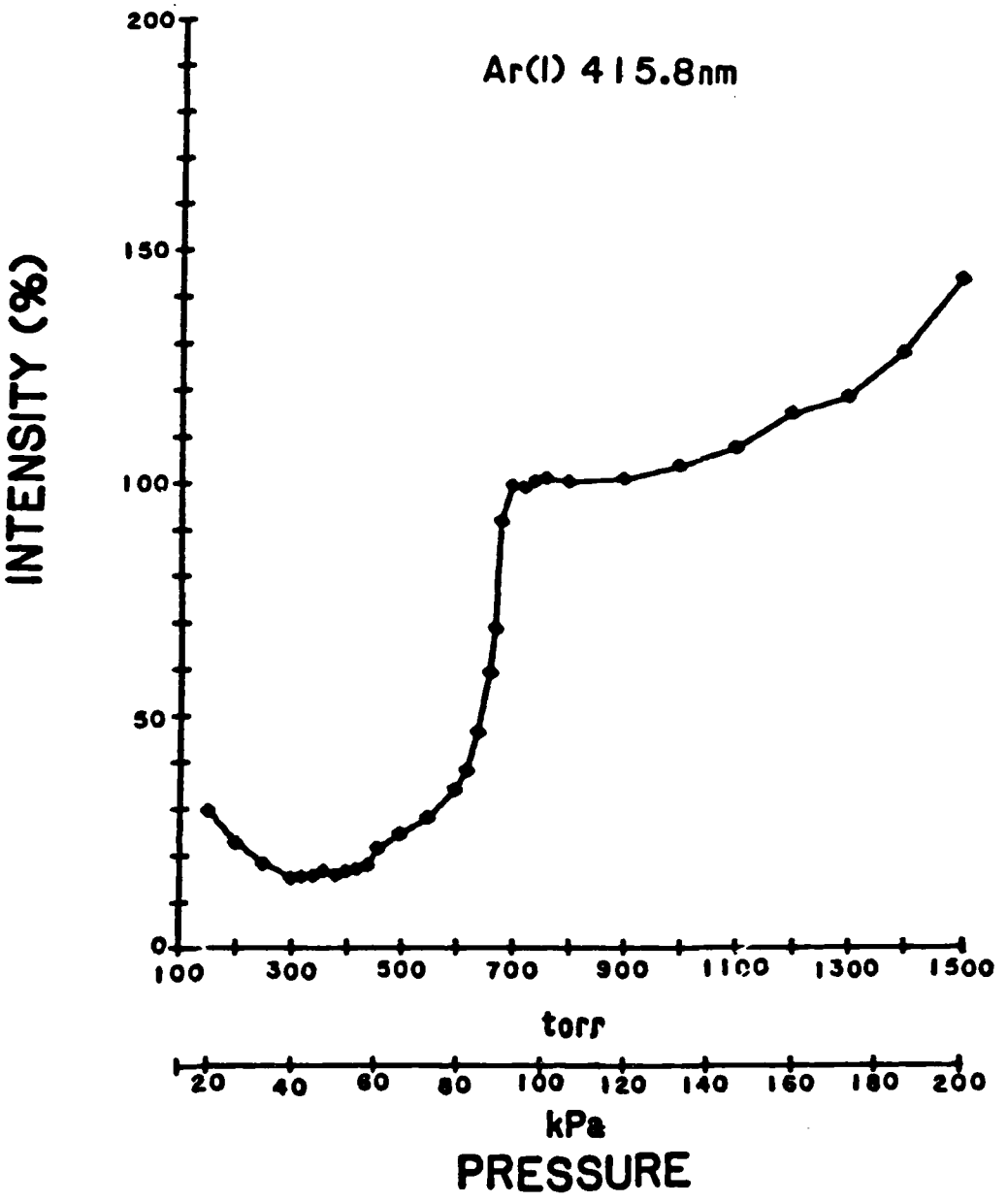

Figure 19

Plot of Ar(I) 415.8 nm emission line intensity vs. torch operating pressure, normalized to 100% intensity at atmospheric pressure.

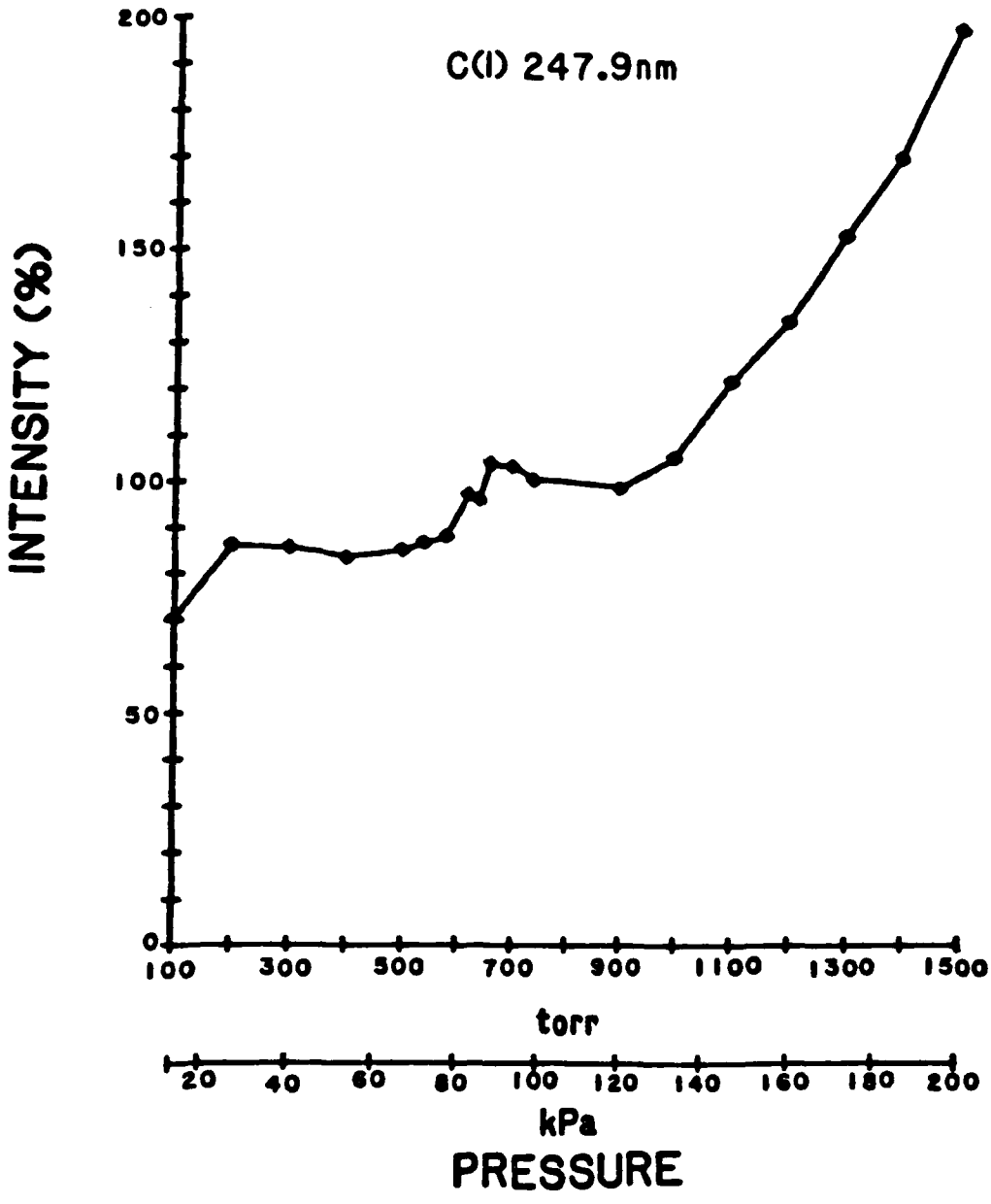

Figure 20

Plot of C(I) 247.9 nm analyte emission line intensity vs. torch operating pressure, normalized to 100% intensity at atmospheric pressure.

These studies have taken the form of a series of experiments, at a variety of torch pressure, determining the electron density and electron temperature by methods independent of assuming LTE and by methods that assume LTE conditions.

LTE electron densities have been determined by stark broadening of the hydrogen beta 486.13 nm line. Stark broadening of the hydrogen beta line has been commonly used for electron density determination within inductively coupled plasmas and is well documented [75-77]. The technique requires a monochromator of only moderate resolving power. The disadvantage of this method is that it does require perturbing the plasma by introduction of a source of hydrogen, usually H_2O.

The distribution of various species within the plasma has also been studied by spatial mapping of the plasma as a function of pressure. Spectroscopic investigations have been carried out on an argon inductively coupled plasma operating at non-atmospheric pressure. The relationship between torch pressure and a number of plasma operating characteristics was explored for torch pressures between 100 and 3000 torr. The plasma operating characteristics examined include observed analyte emission intensities, electron densities, ion to atom ratios, and the deviation of plasma conditions from local thermodynamic equilibrium.

The effect of pressure on the observed analyte emission intensities was found to include factors in addition to the change in density of species within the torch. Emission lines originating from ions and atoms with high ionization potentials (greater than 7 eV) increased in intensity with increasing torch pressure, in excess of that predicted by the increase in density of species present. Conversely, emission lines originating from atoms of low ionization potential decreased in intensity with increasing

torch pressure despite the increase in density. The results of the spatial determination of electron densities and ion to atom ratios indicate that excitation conditions within the central channel of the plasma are shifted towards conditions of local thermodynamic equilibrium as the pressure within the torch is increased. In addition, it is possible to obtain improved limits of detection by optimizing the torch pressure for the analyte element of interest.

SELECTIVE PHOTOIONIZATION FOR MASS SPECTROMETRIC ANALYSIS OF COMPLEX MIXTURES

Trace analysis of compounds in complex matrices is one of the most challenging problems in chemical analysis. Many typical "real world" analytical problems fall into this category. Lacking a technique with sufficient selectivity to probe a molecule of interest without interference from matrix components, the analyst is virtually always faced with the necessity of separating the analyte from these interferents prior to the analysis. For very complex samples, such as coal tars, foodstuffs, or biological samples, this is usually a difficult and tedious procedure. Mass spectrometry is one of the most sensitive probes available for trace analysis, but since the common techniques for producing ions for mass analysis have little or no selectivity, its applicability to real world mixture analysis is impaired by the time and effort involved in the separation step. Gas Chromatography—Mass Spectrometry (GC/MS) has become a powerful tool for dealing with this problem, but the need still remains for more selective ion sources, to reduce the sample clean-up requirement.

One approach to selectivity in ionization is photoionization. The basis of this approach lies in the utilization of the different ionization energies of mixture components, to ionize a small fraction of compounds from a mixture with high efficiency. The ionized components can then be analyzed mass spectrometrically, while the remainder of the mixture is pumped away as neutral molecules. Photoionization mass spectrometry has been used for some time in the study of highly excited states and ionization phenomena in atoms and molecules. The major impediment to the the use of the technique for analytical purposes has been poor sensitivity, due to the low intensity of vacuum ultraviolet radiation available from conventional discharge lamp sources. This type of source has been used with success in sensitive photoionization detection of gas chromatographic effluents at atmospheric pressure. In this case, the high density of carrier gas molecules serves to increase the average residence time of analyte in the radiation beam by collisional confinement, resulting in enhanced photoionization efficiency. (See section on Atmospheric Photoionization.) In the rarified environment of a mass spectrometer ion source at high vacuum, analyte molecules move freely through the ionization volume at thermal velocities, and average residence time in the beam is thus very much smaller. In this case, increased photoionization efficiency can only be brought about by increasing the intensity of ionizing radiation. The advent of high-power lasers has made available the radiation intensity necessary to overcome this problem, and has led to a renewed interest in photoionization as a source for analytical mass spectrometry [78].

Selective and sensitive photoionization mass spectrometry can be accomplished using a variety of strategies. The ability of resonance-enhanced multiphoton ionization to discriminate chemically similar molecules in a

simple mixture has been demonstrated [79]. A second approach is to use nonresonant photoionization to ionize all compounds whose ionization potentials lie below a threshold value determined by the photon energy. This can be accomplished using a nonresonant multiphoton [80,81] or single photon process. Single photon ionization requires radiation in the vacuum ultraviolet (VUV) region, since the ionization potentials of most organic molecules lie in the range 7-14 eV.

Since the first report of laser action in H_2 [82,83], single-step photoionization using a VUV H_2 laser has been reported in a number of laboratories [84-87]. Ion current produced by the laser has been reported to exceed that for a conventional H_2 discharge lamp by a factor of 10^5 [87]. Two-step photoionization has also been demonstrated, in which the H_2 laser was used to ionize a number of molecules from intermediate states excited with a N_2 laser [86,87]. The use of the H_2 laser to produce ions for mass analysis was first reported by Potapov et al. [88] for methylaniline and dimethylaniline.

Evaluation of the H_2 laser photoionization technique as a selective source for analytical mass spectrometry has recently been made in our laboratory [22,89]. The experimental system used in this study is shown in Figure 21 and consists of the laser, coupled with a simple linear time-of-flight mass spectrometer. This mode of mass analysis allows the acquisition of an entire mass spectrum on each laser pulse, in contrast with scanning systems based on magnetic sector and quadrupole instruments. This work has demonstrated great potential for application in the area of trace analysis of pharmacologically-active compounds in biological matrices. The aim of the studies described in this research proposal will be to exploit this

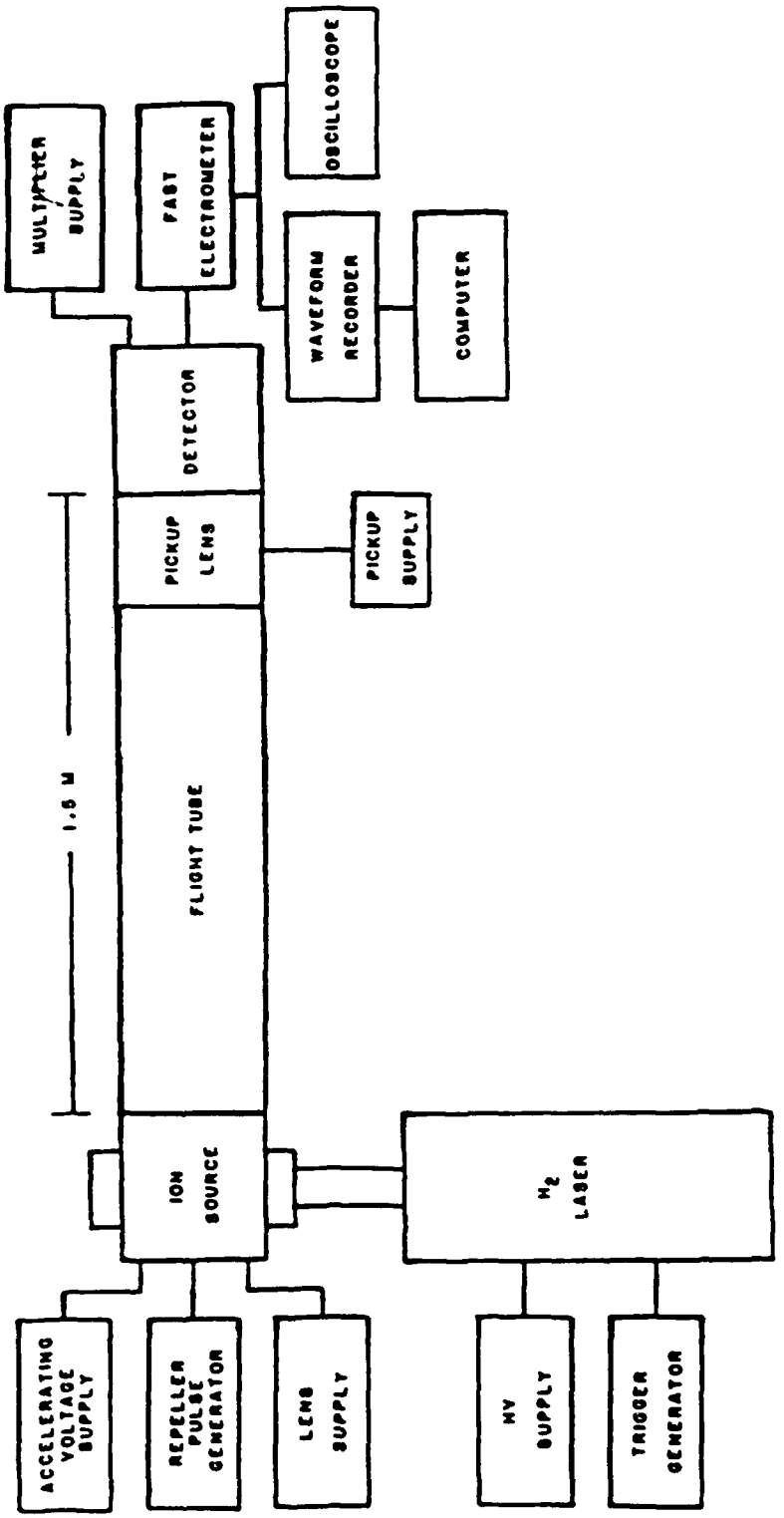

Figure 21
Hydrogen laser/ time of flight mass spectrometer system.

potential through better understanding of the techniques capabilities and the development of methods for analysis of specific drugs and metabolites.

Progress to Date

A list of compounds which have been ionized by the H_2 laser in our laboratory is given in Table 3. In general, the types of organic compounds ionized below 7.8 eV are composed of aromatic amines, secondary and tertiary aliphatic amines, nitrogen-containing heterocycles, polynuclear aromatic hydrocarbons (PAH's), and a number of other compounds which have stabilized molecular ions. Easily ionized nitrogen compounds are trivalent with a largely nonbonding lone electron pair. Substitution by electron-donating groups enhances the ease of ionization. The hydrocarbons have extended systems to stabilize the ion. A number of analytically interesting species fall into these categories, including many pharmaceuticals and drugs of abuse. Selective ionization is particularly interesting for these compounds, since analytical samples typically occur in complex biological matrices such as blood serum and urine. Additionally, nearly all polynuclear aromatic hydrocarbons with three or more rings have ionization potentials below 7.8 eV. These species are of particular interest for environmental samples since many of the compounds are carcinogenic.

The H_2 laser pulse energy is currently about 30 μJ over a series of lines in the 150-160 nm region, with a duration of 0.9 nsec. Since the beam is focused only to the extent necessary to permit a clear transit through the ion source, the energy density is insufficient for production of multiphoton ionization events at an observable level. Under these conditions, the "two-ladder" process [90] leading to fragmentation observed in multiphoton ionization experiments is inoperative. Furthermore, for molecules

Table 3

	Compound	Formula	IP(eV)
Amines:	triethylamine	$C_6H_{15}N$	7.5
	tri-n-propylamine	$C_9H_{21}N$	7.2
	tri-n-butylamine	$C_{12}H_{27}N$	---
	tri-n-hexylamine	$C_{18}H_{39}N$	---
	diphenylamine	$C_{12}H_{11}N$	7.3
	aniline	C_6H_7N	7.7
	N,N-dimethylaniline	$C_3H_{11}N$	7.2
	p-bromo-N,N-dimethylaniline	$C_8H_{10}NBr$	7.3
	4-aminobiphenyl	$C_{12}H_{11}N$	7.5
N-heterocycles:	indole	C_8H_7N	7.8
	1,2,3,4-tetrahydroquinoline	$C_9H_{11}N$	7.6
	carbazole	$C_{12}H_9N$	7.2
	phenothiazine	$C_{12}H_9NS$	7.7
	promazine	$C_{17}H_{20}N_2S$	7.2
	promethazine	$C_{17}H_{20}N_2S$	7.3
	methdilazine	$C_{18}H_{20}N_2S$	7.3
	trimeprazine	$C_{18}H_{22}N_2S$	7.3
	chlorpromazine	$C_{17}H_{19}NSCl$	7.4
PAH:	azulene	$C_{10}H_8$	7.4
	acenapthene	$C_{12}H_{10}$	7.7
	anthracene	$C_{14}H_{10}$	7.5
	phenanthrene	$C_{14}H_{10}$	7.8
Other:	p-dimethoxybenzene	$C_8H_{10}O_2$	7.7

studied thus far the photon energy of 7.8 eV results in transitions into the ionization continuum (or into autoionizing states) which are on the order of 0.1-0.6 eV above the ionization potential (IP). It is expected, therefore, that molecular ions will be formed in their ground electronic state. For large molecules, direct transitions into the ion ground state are generally accompanied by little vibrational excitation, and therefore channels producing fragment ions are not active [91]. For all compounds studied to date, the photoion signals observed consist only of parent molecular ions.

Selectivity of the photoionization process itself is very high. For example, the spectrum resulting from venting a small portion of an injection of a 50% (by volume) mixture of diethylamine and triethylamine (IP's of 8.0 and 7.5 eV, respectively) shows a strong signal for the triethylamine, while the diethylamine is completely rejected. Photoactive compounds currently can be introduced into the ion source through a heated inlet system as dilute solutions in organic solvents, without interference from the solvent.

The selectivity of the single-photon ionization process and the lack of ion fragmentation greatly simplify the spectra of complex "real world" mixtures. This has been demonstrated for simple solvent extracts of foodstuffs such as brewed coffee, soy sauce, and beer, and of biological samples such as urine and blood serum. The biological samples were spiked at the 100 ppb, a clinically realistic level, with several phenothiazine tranquilizers prior to the extraction. Selective photoionization of these extracts yields clear spectra of the spike compounds, which are free of signals due to the matrix.

Comparison with Multiphoton Techniques

H_2 laser photoionization is a threshold ionization technique which will ionize all compounds in a mixture whose ionization potentials lie below the photon energy. Since only parent molecular ions are produced, there is a one-to-one correspondence between peaks observed and compounds ionized. Thus, an interpretable spectrum is obtained, even in the case of a mixture with a number of easily ionized components. On the other hand, nonresonant multiphoton ionization generally results in fragmentation of the parent ion, producing spectra that resemble those from low-energy electron impact [81]. This can easily lead to a confusing spectrum in the same case.

Resonance-enhanced multiphoton ionization requires retuning of the ionizing radiation for each compound ionized. It is possible to obtain parents-only ionization by this approach, by using a low energy density (i.e., low laser power). In general, the power necessary to accomplish this appears to vary with the molecule [79], and so it will likely be necessary to adjust not only the wavelength, but also the laser power for each compound analyzed, in order to obtain soft ionization. The H_2 laser itself is a "superradiant" device which has no mirrors to align. It is inexpensive to build and easy to operate, compared with the high-power tunable dye laser systems required for resonant multiphoton ionization. H_2 laser photoionization is, however, limited to easily ionized compounds, and is not capable of isomer discrimination. Because of the lack of fragmentation in the single-photon ionization process, structural information is not obtained. It should be possible to induce fragmentation by auxiliary mechanisms, if desired (see below).

Analysis of PAH's and Pharmacologically Active Species

As already mentioned, the types of compounds accessible by the H_2 laser photoionization technique include many pharmacologically-active species, including a large number of pharmaceuticals and drugs of abuse. Some examples of drugs which are good candidates for analysis by this technique are shown in Figures 22 and 23. Very little data exist on the ionization potentials of these compounds. Thus, it has been necessary to determine their ionizability in this system experimentally on an individual basis.

Drugs are typically excreted in the form of relatively small amounts of the parent compound, with larger amounts of metabolites. When the metabolism process leaves intact the functionalities associated with easy ionizability of the parent, it should be possible to also observe the metabolites in the spectrum, which will produce a "fingerprint" to enable a clear identification of the drug ingested. In certain cases analysis of the concentrations of various metabolites should be useful in indicating the original dose level and some idea of the time since ingestion (clearly the various metabolic rates vary with individual but even a semiquantitative estimate could be useful in many cases). For example, in the case of cocaine, clinical studies have indicated that 25-40% of the ingested drug is excreted as the principal metabolite, benzoylecgonine, in the urine [92]. A time-course study of the urinary excretion of benzoylecgonine followed by nasal ingestion of cocaine in humans showed the appearance of benzoylecgonine in 1-4 hrs and a peak concentration of this metabolite in urine at 10-12 hours. Wallace et al. applied G.C. analysis to urine samples where patients received cocaine as an anesthetic agent [93]. Eight hours after drug intake, observed concentration ranges of 10 - 124 μg/ml and 0 - 3 μg/ml were reported for benzoylecgonine and cocaine respectively. A significant

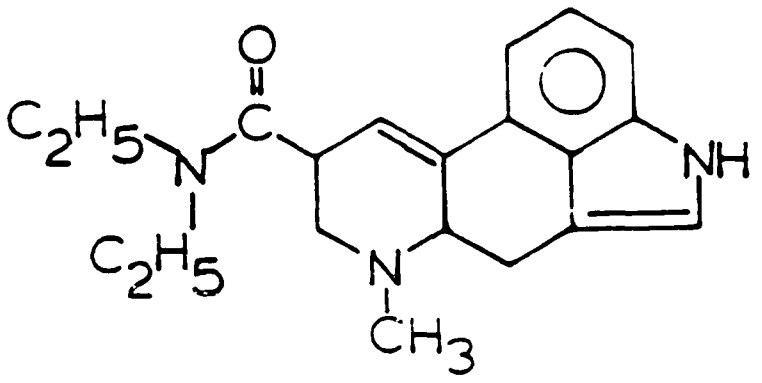

LSD

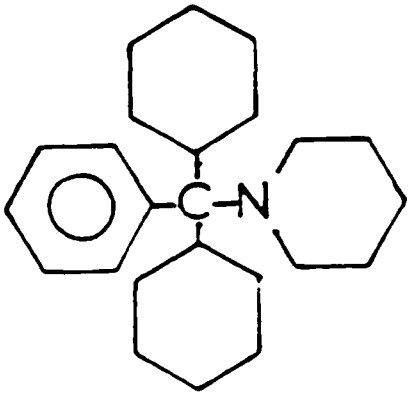

phencyclidine

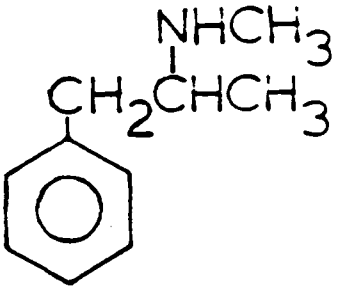

methamphetamine

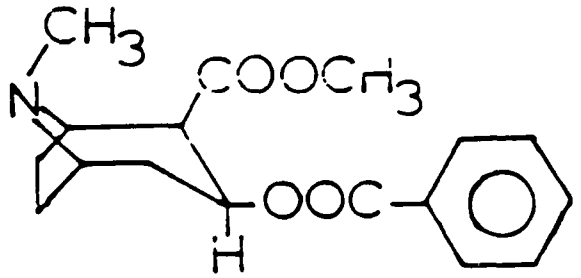

cocaine

Figure 22

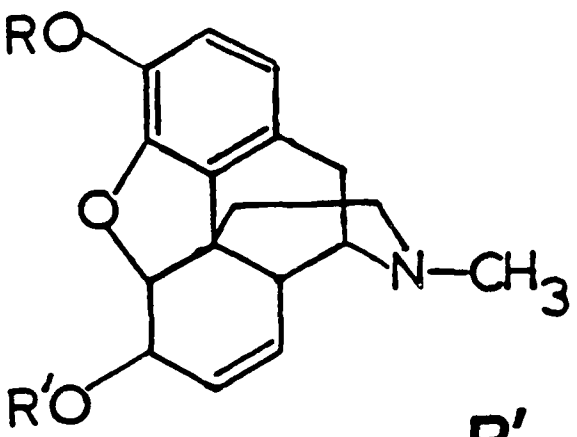

R'	R	compound
H	H	morphine
$COCH_3$	$COCH_3$	heroin
CH_3	H	codeine

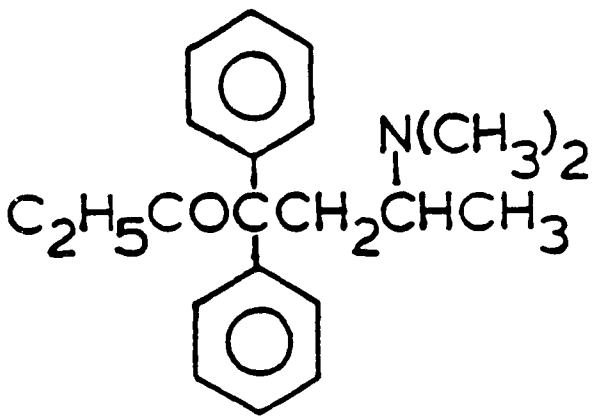

methadone

Figure 23

level (up to 44 μg/ml) of benzoylecgonine was detected in the urine 24 hours after ingestion. However, no cocaine was detected by G.C. analysis in the urine for any of the patients after 25 hours. Wallace et al. reported that 23 individuals not receiving cocaine yielded an average urine blank of 0.14 μg/ml for benzoylecgonine. This demonstrates the need for an alternative technique which is more sensitive and less subject to interferences.

H_2 laser photoionization mass spectrometry has advantages that make it particularly attractive for rapid, trace level screening for drugs of abuse. The instrumentation required could be put into mass production and is relatively inexpensive to build and simple to operate. The size and portability could also be greatly improved through utilization of three dimensional quadrupole ion traps or miniaturized ion cyclotron resonance (ICR) mass analyzers. Speed of analysis is enhanced by the ability to introduce samples by solution injection, as well as by the greatly reduced level of sample pretreatment required. The use of precolumns packed with a hydrophilic polymer has been reported for direct injection of aqueous samples in gas chromatography [94]. The use of such a device in the present system could provide a further substantial speed increase, offering the possibility of direct injection with no pretreatment.

A detailed evaluation of the quantitative aspects of H_2 laser photoionization mass spectrometry has been impractical until recently because of the photographic method of data acquisition used. The level of 100 ppb of phenothiazines used in the previous biological matrix study is well within the "therapeutic window" for chlorpromazine estimated by Curry [95]. It is clear, therefore, that the sensitivity is fully sufficient for determination of at least one class of easily ionized drug compounds at physiologically meaningful levels. Recently, a digital oscilloscope has been added to the

system to acquire mass spectra with computer control via an IEEE-488 interface. The oscilloscope is capable of averaging spectra over one to 256 laser pulses without sacrificing the ability to record the full mass spectrum on each laser pulse. Detection limits have been determined for a group of several polynuclear aromatic hydrocarbons. The ability to average spectra over many laser pulses has resulted in an improvement in detection limits for solid residues and solution injections of photoactive species. Detection limits for polynuclear aromatic hydrocarbons are on the order of 20-50 ng. However, calculations of detector gain based on measured ion current values reveal that the gain can be no greater than 10^6. Additionally, the two stage preamp used to boost the ion signal has been established as the limiting factor in detection of ions. Therefore, the system can be greatly improved through the use of new high gain, multichannel plate detectors. Three-stage multichannel plate detectors have gains as high as 10^9, eliminating the need for further amplification. It is estimated that the use of such a device would improve detection limits of PAH's by 3 orders of magnitude. Such an improvement would give more than adequate sensitivity for analysis for PAH's in environmental samples. With the ability to average mass spectra over a larger number of laser pulses, new digital oscilloscopes capable of averaging up to a million waveforms will yield an even greater improvement in detection limits.

Fundamental knowledge gained with the TOF mass analyzer should prove very useful in assessing the technique's value as a possible selective ion source with other types of mass spectrometers. The ion trap concept holds the additional promise of allowing trapping ions produced from numerous laser pulses before actually measuring the masses of the trapped ions. The

selectivity of the laser ionization technique will significantly reduce the number of matrix ions trapped resulting in vastly improved detection limits.

The information available in the H_2 LPMS experiment can also be greatly expanded by the use of a Fourier transform ICR system for mass analysis. This method inherently lends itself to use with pulsed ion formation. The technique is capable of making exact mass measurements, enabling the determination of the elemental composition of molecular ions. Collision-induced decomposition for determination of the mass spectra of primary ions in an FTMS system has been reported [96].

Ultimately, it will be desirable to evaluate the technique with other types of mass spectrometers.

REFERENCES

1. R.C. Fry and M.B. Denton, Anal. Chem. 49 (1977) 1413.
2. R.C. Fry and M.B. Denton, Appl. Spectrosc. 33 (1979) 393.
3. D.L. Windsor and M.B. Denton, Appl. Spectrosc. 32 (1978) 366.
4. D.R. Heine, Ph.D. Dissertation, University of Arizona (1981).
5. D.L. Windsor, D.R. Heine and M.B. Denton, Appl. Spectrosc. 33 (1979) 56.
6. M.B. Denton, D.L. Windsor, and D.R. Heine, United State Patent No. 4,266,113, May 5, 1981.
7. R.C. Fry and M.B. Denton, D.L. Windsor, and S.J. Northway, Appl. Spectrosc. 33 (1979) 399.
8. D.L. Windsor and M.B. Denton, J. Chrom. Sci. 17 (1979) 492.
9. D.L. Windsor and M.B. Denton, Anal. Chem. 51 (1979) 1116.
10. D.L. Windsor and M.B. Denton, United States Patent No. 4,293,220, October 6, 1981.
11. D.R. Heine, J.S. Babis and M.B. Denton, Appl. Spectrosc. 34 (1980) 595.
12. H.A. Lewis and M.B. Denton, J. Auto. Chem. 3 (1981) 9.
13. J.S. Babis, Ph.D. Dissertation, University of Arizona (1982).
14. J.D. Algeo, D.R. Heine, H.A. Phillips, F.B.G. Hoek, M.R. Schneider, J.M. Freelin and M.B. Denton, Spectrochim. Acta 40B (1985), 1447.
15. D.R. Heine, T.D. Schlabach, and M.B. Denton, Anal. Chem. 54 (1982) 81.
16. J.D. Algeo and M.B. Denton, Appl. Spectrosc. 35 (1981) 35.
17. B.D. Webb and M.B. Denton, Spectrochim. Acta, in press.
18. S.B. Tilden, Ph.D. Dissertation, University of Arizona (1982).
19. P.E. Miller, Ph.D. Dissertation, University of Arizona (1985).
20. T.R. Smith and M.B. Denton, Spectrochim. Acta 40B (1985) 1227.

21. R.S. Aikens, P.M. Epperson and M.B. Denton, SPIE Proc. 501 (1984).

22. T.C. Huth and M.B. Denton, Internat'l. J. Mass Spec. & Ion Proc. 67 (1985) 199.

23. P.M. Epperson, R.D. Jalkian, and M.B. Denton, Anal. Chem. 61 (1989) 282.

24. R.D. Jalkian and M.B. Denton, Appl. Spectrosc. 42(7) (1988) 1194.

25. J.V. Sweedler, R.D. Jalkian, R.S. Pomeroy, and M.B. Denton, Spectrochim. Acta 44B (1989) 683.

26. R.D. Jalkian, R.S. Pomeroy, J.D. Kolczynski, M.B. Denton, J.M. Lerner, and R.E. Grayzel, American Laboratory 21 (1989) 80.

27. P.M. Epperson and M.B. Denton, Anal. Chem. 61 (1989) 1513.

28. J.V. Sweedler and M.B. Denton, Appl. Spectrosc. 43 (1989) 1378.

29. J.V. Sweedler, R.D. Jalkian, and M.B. Denton, Appl. Spectrosc. 44 (1990) 14.

30. M.B. Denton, J. Algeo, S.B. Tilden, Proceedings of the Sixth International Pyrotechnic Seminar, Denver Research Institute (1978).

31. R.C. Fry, S.J. Northway, and M.B. Denton, Anal. Chem. 50 (1978) 1719.

32. M.B. Denton, Yearbook of Science and Technology, McGraw-Hill, New York (1979).

33. R.C. Fry and M.B. Denton, Anal. Chem. 51 (1979) 266.

34. R.B. Bilhorn and M.B. Denton, ONR Tech. Rpt. No. 42, November 25, 1985.

35. J.R. Janesick, T. Elliot, S. Collins, H. Marsh, SPIE 501 (1) (1984) 2.

36. R.W. Simpson, Rev. Sci. Instru. 50 (1979) 730.

37. M.B. Denton, H.A. Lewis, and G.R. Sims, ACS Symp. Ser. No. 236 (Multichannel Image Detect., V. 2 (1983), 133.

38. G.R. Sims and M.B. Denton, ACS Symp. Ser. No 236 (Multichannel Image Detect., V. 2 (1983) 117.

39. E.L. Dereniak and D.G. Crowe, Optical Radiation Detectors John Wiley, New York (1984), Ch. 9.

40. G.R. Sims and M.B. Denton, ONR Tech. Rpt. No. 40, November 25, 1985.

41. R.B. Bilhorn and M.B. Denton, ONR Tech. Rpt. No. 42, November 25, 1985.

42. T. Okamoto, S. Kawata, S. Minami, Appl. Optics 23 (2) (1984) 29.

43. G. Vanesse and H. Sakai, Progress in Optics, V. 6, E. Wolfe, ed., North Holland, New York (1967).

44. Y. D'Astous and M. Blanchard, Am. J. Phys. 50 (5) (1982) 464.

45. S. Kawata, K. Minami and S. Minami, Appl. Optics 22 (22) (1983) 3593.

46. J.R. Janesick, T. Elliot, H.H. Marsh, S. Collins, J. McCarthy, M. Blouke, Rev. Sci. Instru. 56 (5) (1985) 796.

47. Handbook of Spectral Line Characteristics for the DC Plasma/Echelle Systems, Spectrametrics, Inc. (1982).

48. K.G. Michlewicz and J.W. Carnahan, Anal. Chem. 57 (1985) 1092.

49. S. Sprague and W. Slavin, Atomic Abs. Newslett. 12, 20 (1963).

50. J.A. Burrows, J.C. Heerdt, and J.B. Willis, Anal. Chem. 27 (1965) 579.

51. J. Illien, Rapid Methods for the Analysis of Used Oils, Scientific Publications, Broseley, England (1973), p. 70.

52. E.A. Means and D. Ratcliff, Atomic Abs. Newslett. 4 (1965) 174.

53. J.H. Taylor, T.T. Bartels, and N.L. Crump, Anal. Chem. 43 (1971) 1780.

54. J.R. Brown, C.S. Saba, W.E. Rhine, and K.J. Eisentraut, Anal. Chem. 52 (1980) 2365.

55. H.A. Braier, Anal. Chem. 47 (1975) 199R.

56. J.D. Algeo, D.R. Heine, H.A. Phillips, F.B.G. Hoek, M.R. Schneider, J.M. Freelin, and M.B. Denton, Spectrochim. Acta 40B (1985) 1447.

57. M. Ibrahim, W. Nisamaneepong, and J. Caruso, J. Chromatogr. Sci. 23 (4) (1985) 144.

58. M. Ibrahim, W. Nisamaneepong, and J. Caruso, Spectromchim. Acta 40B (1-2) (1985) 367.

59. W. Nisamaneepong, D.L. Haas, and J.A. Caruso, Spectrochim. Acta 40B (1-2) (1985) 3.

60. L.R. Layman and F.E. Lichte, Anal. Chem. 54 (4) (1982) 638.

61. R.J. Lovett, Spectrochim. Acta 37B (1982) 969.

62. P.W.J.M. Boumans and F.L. De Baer, Spectrochim. Acta 32B (1977) 365.

63. M.W. Blades and G.M. Hieftje, Spectrochim. Acta 37B (1982) 191.

64. P.D. Scholz and T.P. Anderson, JQSRT 8 (1968) 1411.

65. A.D. Stokes, J. Phys. D: Appl. Phys. 4 (1971) 916.

66. A.D. Stokes, J. Phys. D: Appl. Phys. 4 (1971) 931.

67. L.N. Medgyesi-Mischang and R.A. Hefferlin, JQSRT 12 (1972) 1627.

68. B.L. Caughlin and M.W. Blades, Spectrochim. Acta 39B (1984) 1583.

69. D.C. Schram, I.J.M.M. Raaymakers, B. van der Sijde, H.J.W. Schenkelaars, and P.W.J.M. Boumans, Spectrochim. Acta 38B (1983) 1545.

70. N. Furuta and G. Horlick, Spectrochim. Acta 37B (1982) 53.

71. P.W.J.M. Boumans, Spectrochim. Acta 37B (1982) 75.

72. R.M. Barnes and R.G. Schleicher, Spectrochim. Acta 36B (1981) 81.

73. P.W.J.M. Boumans and F.J. DeBoer, Spectrochim. Acta 32B (1977) 365.

74. J.B. Gerardo and J.T. Verdeyen, Appl. Phys. Lett. 3 (1963) 121.

75. W.L. Wiese, Plasma Diagnostic Techniques. Eds. R.H. Huddlestone and S.L. Leonard. Academic Press, New York (1965), Ch. 6.

76. H.R. Griem, Plasma Spectroscopy. McGraw-Hill, New York (1964).

77. H.R. Griem, Spectral Line Broadening by Plasmas. Academic Press, New York (1974).

78. R.J. Cotter, Anal.Chem. 56 (1984) 485A-502A.

79. D.M. Lubman and M.J. Kronick, Anal. Chem. 54 (1982) 660-665.

80. V.S. Antonov, V.S. Letokhov and A.N. Shibanov, Appl. Phys. 22 (1980) 293-297.

81. M. Seaver, J.W. Hudgens and J.J. DeCorpo, Int. J. Mass Spectrom. Ion Phys. 34 (1980) 159-173

82. R.T. Hodgson, Phys. Rev. Lett. 25 (1970) 494-497.

83. R.W. Waynant, J.D. Shipman, Jr., R.C. Elton, and A.W. Ali, Appl. Phys. Lett. 17 (1970) 383-384.

84. M. Wacogne, F. Piuzzi, and R. Botter, Bull. Inf. Sci. Tech. Commiss. Energ. At. Fr. 205 (1975), 39.

85. S.V. Andreyev, V.S. Antonov, I.N. Knyezev, V.S. Letokhov and V. G. Movshev, Phys. Lett. 54A (1975) 91-92.

86. V.S. Antonov, I.N. Knyazev, V.S. Letokhov and V.G. Movshev, Sov. Phys. JETP 46 (1977) 697-704.

87. V.S. Antonov, I.N. Knyazev, V.M. Matiuk, V.G. Movshev, V.K. Potapov, Opt. Lett. 3 (1978) 37-39.

88. V.K. Potapov, V.G. Movshev, V.S. Letokhov, I.N. Knyazev, and T.I. Evlasheva, Sov. J. Quantum Electron. 6 (1976), 1437.

89. T.C. Huth and M.B. Denton, Analytica Chimica Acta, submitted for publication.

90. U. Boesl, H.J. Neusser and E.W. Schlag, J. Chem. Phys. 72 (198.) 4327-4333.

91. H.M. Rosenstock, K. Draxl, B.W. Steiner and J.T. Herron, J. Phys. Chem. Ref. Data 6 (1977) Suppl.1.

92. R.L. Foltz, A.F. Fentiman, and R.B. Foltz, "Cocaine and Its Major Metabolite Benzoylecgonine," Ch. 7 in GC/MS Assays for Abused Drugs in Body Fluids, National Institute on Drug Abuse Research Monograph Series No. 32, Department of Health and Human Services (1980), p. 90.

93. J.E. Wallace, H.E. Hamilton, D.E. King, D.J. Bason, H.A. Schwertner, and S.C. Harris, Anal. Chem. 48 (1976) 34.

94. Reference on use of Nafion precolumns for aqueous sample injection in GC; see Klaus Stetzenbach at UAC for this.

95. S.H. Curry, Psychopharmacol. Commun. 2 (1976), 1.

96. R.B. Cody, R.C. Burnier, and B.S. Freiser, Anal. Chem. 54 (1982), 96.

Publications

1. B.D. Webb and M.B. Denton, "Comparison of a Very High Frequency 148 MHz Inductively Coupled Plasma with a 27 MHz ICP," Spectrochim. Acta 41B(4), 361 (1986).

2. P. E. Miller and M. B. Denton, "The Quadrupole Mass Filter: Basic Operating Concepts," J. Chem. Ed. 63 617 (1986).

3. J.S. Babis, Jerrold M. Kacsir and M.B. Denton, "Glass Capillary Array Nebulizer for Atomic Spectrometry," Appl. Spec. 43(5), 786 (1989).

4. P.E. Miller and M.B. Denton, "The Transmission Properties of an RF- Only Quadrupole Mass Filter," Int. J. Mass Spectrom. & Ion Proc. 72, 223 (1986).

5. T.R. Smith, Hugh A. Phillips and M. Bonner Denton, "A Safety Shutoff for Your Plasma Torch Box," Appl. Spec. 41(2), 330 (1987).

6. T.R. Smith and M.B. Denton, "A High Pressure Inductively Coupled Plasma Torch," Appl. Spec. 41(4), (1987).

7. B.D. Webb and M.B. Denton, "Effect of Torch Size on a 148 MHz Inductively Coupled Plasma," J.A.A.S., Vol. 2, No.1, 21-26 (1987).

8. T.C. Huth and M.B. Denton, "Complex Mixture Analysis by Photoionization Mass Spectrometry with a VUV Hydrogen Laser Source," Analytica Chimica Acta 192, 165-173 (1987).

9. M.B. Denton, "Concepts for Improved Automated Laboratory Productivity," The Analyst 112, 347-353 (1987).

10. P.M. Epperson, J.V. Sweedler, M.B. Denton, G.R. Sims, T.W. McCurnin, R.S. Aikens, "Electro-optical Characterization of the Tektronix TK512M-011 CCD," J. Opt. Eng. 26(8), 715-724 (August 1987).

11. G.R. Sims, M.B. Denton, "Spatial Pixel Crosstalk in a Charge Injection Device," J. Opt. Eng. 26(10), 999-1007 (October 1987).

12. G.R. Sims, M.B. Denton, "Characterization of a Charge Injection Device Camera System for Spectrochemical Measurements," J. Opt. Eng. 26(10), 1008-1019 (October 1987).

13. J.V. Sweedler, M.B. Denton, G.R. Sims, R.S. Aikens, "A Single Element Charge Injection Device as a Spectroscopic Detector," J. Opt. Eng. 26(10), 1020-1028 (October 1987).

14. H.A. Phillips, H.L. Lancaster, M.B. Denton, K. Rozsa, and P. Apai, "Self-Absorption in Copper Hollow Cathode Discharges," Proceedings of the Hungarian Academy of Sciences Central Research Institute for Physics, Budapest (1987).

15. R.B. Bilhorn, J.V. Sweedler, P.M. Epperson, M.B. Denton, "Charge Transfer Device Detectors for Analytical Optical Spectroscopy - Operation and Characteristics," Applied Spectroscopy 41(7), 1114-1125 (1987).

16. R.B. Bilhorn, P.M. Epperson, J.V. Sweedler, M.B. Denton, "Spectrochemical Measurements with Multichannel Integrating Detectors," Applied Spectroscopy 41(7), 1125-1136 (1987).

17. M.B. Denton, R.B. Bilhorn, R.S. Pomeroy, J.V. Sweedler, P.M. Epperson, and R.D. Jalkian, "Array Detectors for Plasma Spectrochemistry," ICP Information Newsletter, Vol. 13, p. 64 (1988).

18. P.M. Epperson, J.V. Sweedler, R.B. Bilhorn, G.R. Sims, and M.B. Denton, "Applications of Charge-Transfer Devices in Spectroscopy," Analytical Chemistry 60(4), 327A (1988).

19. J.V. Sweedler, R.B. Bilhorn, P.M. Epperson, G.R. Sims, and M.B. Denton, "High Performance Charge Transfer Device Detectors," Analytical Chemistry 60(5), 282A (1988).

20. H.A. Phillips, H.L. Lancaster, M.B. Denton, K. Rozsa, and P. Apai, "Self-Absorption in Copper Hollow Cathode Discharges: Effects on Spectral Line Shape and Absorption Sensitivity," Applied Spectroscopy 42(4), 572-576 (1988).

21. P.M. Epperson, R.D. Jalkian, and M.B. Denton, "Molecular Fluorescence Measurements with a Charge-Coupled Device Detector," Analytical Chemistry 61, 282 (1989).

22. R.D. Jalkian and M.B. Denton, "Ultra-Trace Level Determination of Cobalt, Chromium, and Hydrogen Peroxide by Luminol Chemiluminescence Detected with a Charge-Coupled Device," Applied Spectroscopy 42(7), 1194-1199 (1988).

23. M.B. Denton, J.M. Freelin, and T.R. Smith, Sample Introduction in Atomic Spectroscopy, Chapter 4 "Ultrasonic, Babington and Thermospray Nebulization," Elsevier Science Publishers, 1988.

24. R.S. Pomeroy, M.B. Denton, N.R. Armstrong, "Voltammetry at the Thin Film Mercury Electrode (TFME): Anodic and Cathodic Stripping Voltammetries and Simple Potentiostat Construction," Journal of Chemical Education 66(10), 877-880 (1989).

25. J.V. Sweedler, R.D. Jalkian, R.S. Pomeroy, and M.B. Denton, "A Comparison of CCD and CID Detection for Atomic Emission Spectroscopy," Spectrochimica Acta 44B(7), 683 (1989).

26. R.B. Bilhorn and M.B. Denton, "Elemental Analysis with a Plasma Emission Echelle Spectrometer Employing a Charge Injection Device (CID) Detector," Applied Spectroscopy 43(1), 1 (1989).

27. R.D. Jalkian, R.S. Pomeroy, J.D. Kolczynski, M.B. Denton, J.M. Lerner, and R.E. Grayzel, "Evaluation and Application of a Holographic Aberration Corrected Imaging Spectrograph," American Laboratory 21(2), 80-88 (1989).

28. R.D. Jalkian and M.B. Denton, "HPLC Determination of Polycyclic Aromatic Compounds by Fluorescence Detected with a Charge-Coupled Device," Society of Photo-Optical Instrumentation Engineers (SPIE) Proceedings 1054 (1989).

29. R.D. Jalkian, K.L. Ratzlaff, and M.B. Denton, "HPLC Determination of Transition Metal Ions by Chemiluminescence Detected with a Charge-Coupled Device," Society of Photo-Optical Instrumentation Engineers (SPIE) Proceedings 1055 (1989).

30. J.D. Kolczynski, R.S. Pomeroy, R.D. Jalkian, and M.B. Denton, "Spatial and Spectral Imaging of Plasma Excitation Sources," Applied Spectroscopy 43(5), 887 (1989).

31. P.M. Epperson and M.B. Denton, "Binning Spectral Images in a Charge-Coupled Device (CCD)," Analytical Chemistry 61, 1513 (1989).

32. J.V. Sweedler, R.D. Jalkian, and M.B. Denton, "A Linear Charge Coupled Device Detector System for Spectroscopy," Applied Spectroscopy 43(6), 953 (1989).

33. J.V. Sweedler and M.B. Denton, "Spatially Encoded Fourier Transform Spectroscopy in the Ultraviolet to Near Infrared," Applied Spectroscopy 43(8), 1378-1384 (1989).

34. T.R. Smith and M.B. Denton, "LTE Conditions Within the Central Channel of the Plasma," Applied Spectroscopy 43(8), 1385-1387 (1989).

35. H.A. Phillips, T.R. Smith, B.D. Webb, and M.B. Denton, "Simplified Construction of Demountable ICP Torches," Applied Spectroscopy 43(8), 1488-1489 (1989).

36. J.V. Sweedler, R.D. Jalkian, and M.B. Denton, "Crossed Interferometric Dispersive Spectroscopy," Applied Spectroscopy 44(1), 14-20 (1990).

37. T.R. Smith and M.B. Denton, "Evaluation of Current Nebulizers and Nebulizer Characterization Techniques," Applied Spectroscopy 44(1), 21-24 (1990).

In Press

1. R.S. Pomeroy, J.V. Sweedler, M.B. Denton, "Charge Injection Device Detection for Improved Performance for Atomic Emission Spectroscopy," Talanta, in press.

2. G.R. Sims and M.B. Denton, "Simultaneous Multielement Atomic Emission Spectrometry Using a Charge Injection Device Detector," Talanta, in press.

3. P.E. Miller and M.B. Denton, "A Notch Rejection Quadrupole Mass Filter," International Journal of Mass Spectrometry and Ion Processes, in press.

4. R.S. Pomeroy, J.D. Kolczynski, J.V. Sweedler, and M.B. Denton, "Analysis of Microgram Amounts of Airborne Particulates by Simultaneous Multiwavelength Atomic Emission Spectroscopy," Mikrochimica Acta, in press.

5. H.A. Phillips, M.B. Denton, K. Rozsa, and P. Apai, "Absorption and Emission of Copper Radiation in Low and High Voltage Hollow Cathode Discharges," Spectrochimica Acta B, in press.

6. R.B. Bilhorn, R.S. Pomeroy, and M.B. Denton, Trace Metal Analysis and Speciation, Chapter 5, "The Future of Intelligent Spectrometers in Speciation by Atomic Emission Spectrometry," Elsevier Science Publishers, in press.

7. M.B. Denton, M.J. Pilon, and J.S. Babis, "Vacuum Ultraviolet Inductively Coupled Plasma Spectroscopy for Element Selective Detection of Nonmetals," Applied Spectroscopy, in press.

Personnel Who Participated in the Research on ONR Contract

Robert B. Bilhorn
Patrick M. Epperson
Thomas R. Smith
Julie M. Freelin
Burton R. Lamoureux
Gary R. Sims
Herbert L. Lancaster
Mark E. Homan
Jeffrey D. Kolczynski
Hugh A. Phillips
Jonathan V. Sweedler
Rafi D. Jalkian
Jeffrey W. Finch
Robert S. Pomeroy
Michael J. Pilon
Mark E. Baker
D. Brooke Hatfield
Marlys J. M. Nesset
David A. Radspinner

Awards Received

1. Plenary Lecturer for the Royal Society of Chemistry SAC-86, University of Bristol, July 20-26, 1986.

2. A Tomas Hirschfeld Scholar Award presented by the Federation of Analytical Chemistry and Spectroscopy Societies to J. V. Sweedler.

3. 1988 Gordon F. Kirkbright Bursary for travel to the National Atomic Spectroscopy Symposium presented by the British National Spectroscopy Society to J. V. Sweedler.

4. Summer Fellowship sponsored by the Society of Analytical Chemists of Pittsburgh to J. V. Sweedler.

5. 1988 McPherson Award in Applied Spectroscopy sponsored by the Society of Applied Spectroscopy to J. V. Sweedler.

6. 1989 ACS Division of Analytical Chemistry Award in Chemical Instrumentation.

Technical Report No. 45: "Electron Impact Phenomena in VUV Photoionization Mass Spectroscopy" by Thomas C. Huth and M. Bonner Denton, May 1987.

Technical Report No. 46: "Concepts for Improved Automated Laboratory Productivity" by M. Bonner Denton, May 1987.

Technical Report No. 47: "A High Pressure Inductively Coupled Plasma Torch" by Thomas R. Smith and M. Bonner Denton, May 1987.

Technical Report No. 48: "A Single Element Charge Injection Device as a Spectroscopic Detector" by J.V. Sweedler, M.B. Denton, G.R. Sims, and R.A. Aikens, May 1987.

Technical Report No. 49: "Charge Transfer Device Detectors for Analytical Optical Spectroscopy - Operations and Characteristics" by R.B. Bilhorn, J.V. Sweedler, P.M. Epperson, and M.B. Denton, May 1987.

Technical Report No. 50: "Spectrochemical Measurements with Multichannel Integrating Detectors" by R.B. Bilhorn, P.M. Epperson, J.V. Sweedler, and M.B. Denton, May 1987.

Technical Report No. 51: "Electro-Optical Characterization of the Tektronix TK512M-011 CCD" by P.M. Epperson, J.V. Sweedler, M.B. Denton, G.R. Sims, T.W. McCurnin, and R.S. Aikens, July 1987.

Technical Report No. 52: "Binning Spectral Images in a Charge-Coupled Device (CCD)" by Patrick M. Epperson and M. Bonner Denton, February 1988.

Technical Report No. 53: "Recent Advances in Optical Spectroscopy Using High Performance Array Detectors" by M.B. Denton, R.B. Bilhorn, P.M. Epperson, and J.V. Sweedler, February 1988.

Technical Report No. 54: "The Effect of Torch Pressure on Analyte Response in a 27 MHz Inductively Coupled Plasma" by Thomas R. Smith and M. Bonner Denton, February 1988.

Technical Report No. 55: "A Revolution in Optical Spectroscopy - High Performance Array Detectors" by M. Bonner Denton, February 1988.

Technical Report No. 56: "The Future of Intelligent Spectrometers in Metal Speciation by Atomic Emission Spectrometry" by M. Bonner Denton and R.B. Bilhorn, February 1988.

Technical Report No. 57: "Self-Absorption in Copper Hollow Cathode Discharges: Effects on Spectral Lineshape and Absorption Sensitivity" by H.A. Phillips, H.L. Lancaster, M.B. Denton, K. Rozsa, and P. Apai, February 1988.

Technical Report No. 58: "Molecular Spectroscopy Using Charge Transfer Device Detectors" by J.V. Sweedler, P.M. Epperson, R.D. Jalkian, and M.B. Denton, February 1988.

Technical Report No. 59: "Comparison of Charge Transfer Device and Photomultiplier Tube Performance for Extremely Low Photon Fluxes" by Jonathan V. Sweedler and M. Bonner Denton, February 1988.

Technical Report No. 60: "The Electromagnetic Spectrum - The Information Mine" by M.B. Denton, R.B. Bilhorn, and J.V. Sweedler, February 1988.

Technical Report No. 61: "Molecular Fluorescence Measurements with a Charge-Coupled Device Detector" by P.M. Epperson, R.D. Jalkian, and M.B. Denton, February 1988.

Technical Report No. 62: "Array Detectors for Plasma Spectrochemistry" by M.B. Denton, R.B. Bilhorn, R.S. Pomeroy, J.V. Sweedler, P.M. Epperson, and R.D. Jalkian, February 1988.

Technical Report No. 63: "Femptogram Level Determination of Cobalt and Chromium by Luminol Chemiluminescence Detected by a Charge-Coupled Device" by R.D. Jalkian and M.B. Denton, February 1988.

Technical Report No. 64: "High Performance Charge Transfer Device Detectors" by J.V. Sweedler, R.B. Bilhorn, P.M. Epperson, G.R. Sims, and M.B. Denton, February 1988.

Technical Report No. 65: "Theoretical Comparison of Dispersive and Interferometric Spectrometer Performance for UV-Vis Spectroscopy" by J.V. Sweedler and M.B. Denton, February 1988.

Technical Report No. 66: "Instrumentation and Techniques for Internal Error Detection in Atomic Emission Spectroscopy" by R.S. Pomeroy and M.B. Denton, February 1988.

Technical Report No. 67: "Spatially Resolved Absorption Measurements of Optically Dense Metal-Phthalocyanine Thin-Films with a Charge-Coupled Device" by P.M. Epperson, T.M. Sims, G.R. Sims, and M.B. Denton, February 1988.

Technical Report No. 68: "Applications of Charge Transfer Devices in Spectroscopy" by P.M. Epperson, J.V. Sweedler, R.B. Bilhorn, G.R. Sims, and M.B. Denton, February 1988.

Technical Report No. 69: "Molecular Spectroscopy Using Charge-Coupled Device Detectors" by J.V. Sweedler, R.D. Jalkian, P.M. Epperson, and M.B. Denton, February 1988.

Technical Report No. 70: "Atomic Spectroscopy with Charge Transfer Devices" by M.B. Denton, R.B. Bilhorn, R.S. Pomeroy, R.D. Jalkian, and M.J. Pilon, February 1988.

LTE Conditions within the Central Channel of the Plasma

THOMAS R. SMITH and M. BONNER DENTON*
Shell Development Co., P.O. Box 1380, Houston, Texas 77251 (T.R.S.); and
University of Arizona, Department of Chemistry, Tucson, Arizona 85721 (M.B.D.)

Studies were performed on the effect of torch pressure on the excitation conditions within an inductively coupled plasma (ICP). Experimentally measured magnesium ion-to-atom ratios and electron densities were used to determine the deviation of the plasma from local thermodynamic equilibrium (LTE) conditions. Results of these studies indicate that the plasma is in an infrathermal state when operated at atmospheric pressure, and excitation conditions within the central channel of an ICP shift towards LTE conditions as torch pressure is increased.

Index Headings: Inductively coupled plasma; Pressure; Local thermodynamic equilibrium; Emission spectroscopy; Electron densities; Ion-to-atom ratios.

INTRODUCTION

The state of a plasma in a closed system can be characterized by measuring a few macroscopic properties such as pressure, temperature, and concentration. Several statistical distribution functions, all of which are sensitive to temperature, relate these macroscopic properties to the microscopic state of the species within the plasma. These distribution functions include: Maxwell, Boltzmann, and Saha distributions and Planck's law.[1]

Maxwell's distribution gives rise to the gas kinetic temperature of a particle (T_{kin}) and the electron temperature (T_e). The population distribution of bound states, energy levels below the next ionization potential of the species, is a function of the Boltzmann distribution. The population of each energy level within an atom or ion is determined by the excitation temperature (T_{exc}). In ICPs, different excitation temperatures are often reported for species in the same location of the plasma.[2] In fact, different excitation temperatures are even reported for different transitions within the same species.[3] Excitation temperatures can be determined from the relative emission intensities of several lines from a given species. The population distribution of ionization products is governed by the Saha expression. The Saha distribution determines the ion-to-atom population ratio for a species as a function of ionization temperature (T_{ion}). The following equation (Eq. 1) relates the ionization temperature of a species to the experimentally observed ion-to-atom emission intensity ratio:

$$\frac{I^+}{I^\circ} = \frac{2(2\pi m_e kT)^{3/2}}{n_e h^3} \frac{g^+ A^+ \lambda^\circ}{g^\circ A^\circ \lambda^+} \exp(-\Delta E/kT) \qquad (1)$$

where I^+ and I° are the intensities for the ionic and atomic emissions; g^+ and g° are the statistical weights of the upper states involved in the emissions; A^+ and A° are the Einstein transition probabilities for spontaneous emission for the transitions; λ^+ and λ° are the wavelengths of the ionic and atomic emissions; k is the Boltzmann constant; h is Planck's constant; m_e is the mass of an electron; ΔE is the energy difference between the upper state of the atomic transition and the upper state of the ionic transition; n_e is the electron density; and T is the ionization temperature.

If the plasma is in a state of Local Thermodynamic Equilibrium (LTE), then $T_{kin} = T_e = T_{exc} = T_{ion}$. However, this has been found to not be the case for an argon atmospheric pressure inductively coupled plasma. To determine the extent of deviation from LTE conditions, one can measure magnesium ion-to-atom ratios and compare them to magnesium ion-to-atom ratios calculated for theoretical (LTE) conditions. The deviation from LTE is expressed as a "b_r" value, which is defined as the observed ion-to-atom ratio divided by the theoretical ion-to-atom ratio:[4]

$$b_r = \frac{(I^+/I^\circ)_{obs}}{(I^+/I^\circ)_{LTE}} . \qquad (2)$$

A b_r value equal to one implies that the plasma is at LTE conditions.

EXPERIMENTAL

Magnesium Ion-to-Atom Ratios. Magnesium ion-to-atom ratios [Mg(II)/Mg(I)] were measured for the central channel of the plasma at a number of different torch pressures. The variable pressure torch and optical periscope described elsewhere[5,6] were used to collect spatial maps of the magnesium emission line. The spatial maps ranged from 5 mm on either side of the center of the plasma and from 8 to 28 mm above the load coil. Data were taken at 1-mm steps horizontally and 2-mm steps vertically. Figure 1 shows the effect of pressure on the maximum observed emission intensity for the Mg(II) 279.553-nm and Mg(I) 285.213-nm emissions. It can be seen that, while both emissions increase in intensity with increasing pressure, the magnesium ion emission appears to increase more rapidly than the magnesium atom emission. A number of workers have reported that the ratio of emission intensities from species in the central channel of the plasma is not affected by the Abel inversion process.[7,8] Therefore, observed emission intensity ratios were used for temperature determinations and ion-to-atom ratio calculations, to minimize computational errors.

The effect of increasing torch pressure on Mg(II)/Mg(I) intensity ratios is shown in Fig. 2. The ion-to-atom ratios are the maximum Mg(II)/Mg(I) ratios observed in the normal analytical zone of the central channel of the plasma. The central channel of the plasma was chosen for study because it is the region one views in order to perform analysis using an ICP.

Received 5 May 1989.
* Author to whom correspondence should be sent.

0003 7028/89/4308-1385$2.00/0

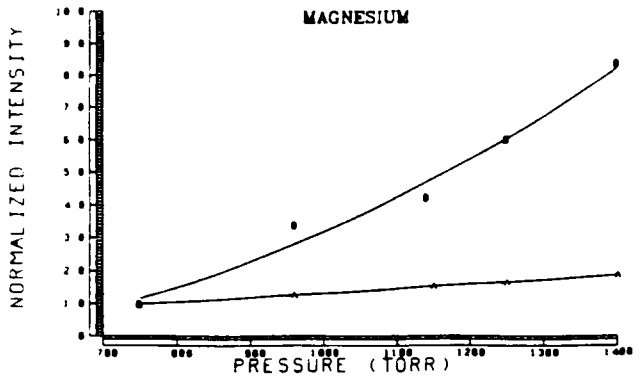

FIG. 1. Plot of emission intensity vs. torch pressure for: (A) Mg(I) 285.213 nm; (B) Mg(II) 279.553 nm. Emission intensities are in analog-to-digital converter units (ADUs).

Emission Line Profile Broadening. Electron densities were measured for the plasma through Stark broadening of the hydrogen beta line (H_β 486.1 nm) emission profile. Water was introduced into the plasma as the source of hydrogen for the broadening determination. The observed broadening was corrected for thermal Doppler broadening and the instrument broadening caused by the monochromator.

Line profiles of the H_β emission were determined by scanning the spectral region from 485.44 to 486.64 nm at 0.02-nm increments. A total of 61 data points were taken per scan. Scans were collected across the plasma at 1-mm positions horizontally and up the plasma at 2-mm positions vertically. The 1-mm × 2-mm grid covered the plasma from 5 mm on either side of the center of the plasma and from 8 mm above the load coil to 28 mm above the load coil. This region included the normal analytical zone of the plasma which was the same region that was used for measuring Mg(II)/Mg(I) ratios in the central channel of the plasma.

Electron Densities and Electron Temperatures. Electron densities were calculated for plasmas operating at a number of different torch pressures. Table I lists the Stark half-widths and electron densities found at the location of the maximum Mg(II)/Mg(I) ratio within the central channel of the plasma. Dalton's law can be combined with the Saha equation to obtain a relationship between electron density, electron temperature, and pressure. This relationship is given by:

$$n_e^2 = \frac{P}{kT_e}\frac{2g^+}{g^\circ}\left(\frac{2\pi m_e kT_e}{h^2}\right)^{3/2}\exp(-\Delta E/kT_e) \qquad (3)$$

where P is the measured torch pressure, and T_e is the electron temperature.

This equation can be used to calculate electron temperatures from the electron density and the torch pressure (see Table I). The calculation of electron temperatures is done in an iterative manner, where LTE conditions within the plasma are assumed. The method of using a single plasma parameter to calculate all of the other parameters under LTE conditions was introduced by Caughlin and Blades.[4] Their approach has the advantage of generating true LTE values for Mg(II)/Mg(I) ratios for comparison to the observed Mg(II)/Mg(I) ratios. Previous approaches used non-LTE values for electron densities and electron temperatures to calculate LTE Mg(II)/Mg(I) ratios, which lead to erroneous results for the deviation of plasma conditions from LTE conditions.

TABLE I. Measured and theoretical values for the region of highest Mg(II)/Mg(I) in the central channel.

Pressure	Stark half-width (nm)	n_e (cm^{-3})	T_e (K)	Mg(II)/Mg(I)		b_r
Measured	Measured	Measured	Calculated	Exp.	LTE	Calculated
750	0.162	7.4×10^{14}	7540	2.1	19.6	0.11
960	0.157	7.1×10^{14}	7440	3.5	17.1	0.20
1150	0.161	7.3×10^{14}	7410	3.8	15.7	0.24
1250	0.203	1.0×10^{15}	7580	4.1	15.6	0.26
1400	0.223	1.2×10^{15}	7630	5.4	14.2	0.38

DISCUSSION

Table I lists the LTE Mg(II)/Mg(I) ratios calculated from Eq. 1 with the observed electron densities and calculated LTE electron temperatures. The b_r values calculated with Eq. 2 are also included in Table I and are plotted against torch pressure in Fig. 3. It can be seen from Fig. 3 that, while the central channel of the plasma is not at LTE conditions at atmospheric pressure, the plasma conditions do shift toward LTE conditions as the torch pressure is increased.

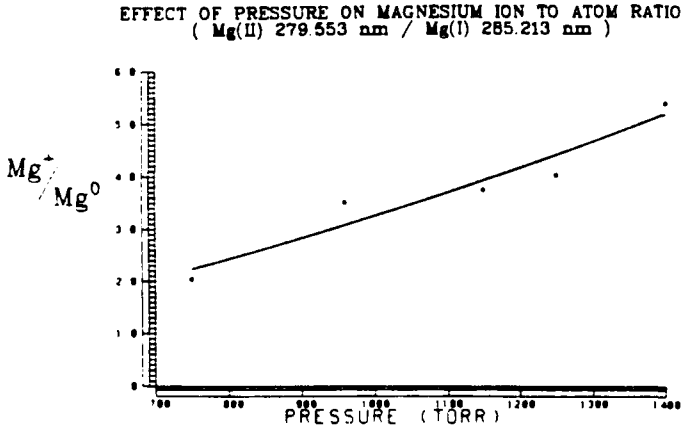

FIG. 2. Plot of magnesium-ion-to-atom ratio vs. torch pressure for the normal analytical zone of the plasma.

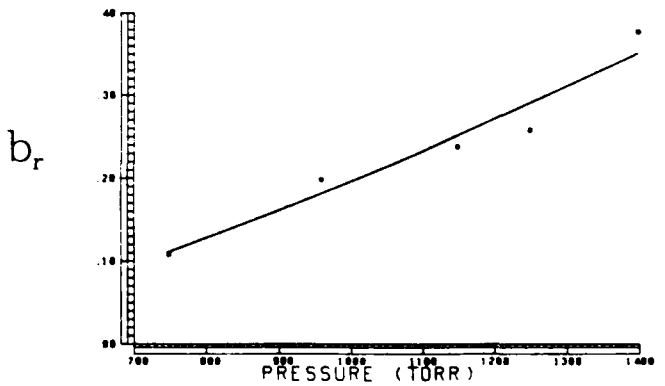

FIG. 3. Plot of b_r values vs. torch pressure for Mg(II) 279.553 nm/Mg(I) 285.213 nm. For the region of maximum ion-to-atom ratio in normal analytical zone of the central channel of the plasma.

CONCLUSION

As the torch pressure is increased above atmospheric pressure, the energy transfer mechanisms within the plasma are becoming collisionally dominated. These results also agree with Blades'[4] evaluation of the plasma as being infrathermal at atmospheric pressure. That is, the higher ionization states of species within the plasma are under-populated relative to the ground state. Thus, as the torch pressure is increased and the plasma shifts toward LTE conditions, the emission (and, therefore, the population of the ionic states) is seen to increase more rapidly than the atomic states. This causes the increase in observed ion-to-atom ratio with increasing pressure.

1. M. W. Blades, "Excitation Mechanisms and Discharge Characteristics: Recent Developments," in *Inductively Coupled Plasma Emission Spectroscopy*, Part 2, P. W. J. M. Boumans, Ed. (Wiley-Interscience, New York 1987).
2. J. Nojiri, K. Tanabe, H. Uchida, H. Haraguchi, K. Fuwa, and J. D. Winefordner, Spectrochim. Acta **38B**, 61 (1983).
3. J. F. Adler, R. M. Bombelka, and G. F. Kirkbright, Spectrochim. Acta **35B**, 163 (1980).
4. B. L. Caughlin and M. W. Blades, Spectrochim. Acta **39B**, 1583 (1984).
5. T. R. Smith and M. B. Denton, Spectrochim. Acta **40B**, 1227 (1985).
6. T. R. Smith, "Excitation Processes within an Inductively Coupled Plasma as a Function of Pressure and Related Studies," Ph.D. Dissertation, University of Arizona, Tucson, Arizona (1988).
7. J. Jarosz, J. M. Mermet, and J. Robin, Spectrochim. Acta **33B**, 55 (1978).
8. B. D. Webb, "Fundamental Investigations of a 148 MHz Inductively Coupled Plasma Discharge," Ph.D. Dissertation, University of Arizona, Tucson, Arizona (1985).